




RESEARCH PAPER

A comprehensive study of monkeypox disease through fractional mathematical modeling

M. Manivel ^{1,‡}, A. Venkatesh ^{1,*,‡} and Shyamsunder Kumawat ^{2,‡}

¹Department of Mathematics, AVVM Sri Pushpam College (Affiliated to Bharathidasan University, Tiruchirappalli), Poondi, Thanjavur 613503, Tamilnadu, India, ²Department of Mathematics, SRM University Delhi-NCR, Sonapat 131029, Haryana, India

*Corresponding Author

‡manivelmani718@gmail.com (M. Manivel); avenkateshmaths@gmail.com (A. Venkatesh); skumawatmath@gmail.com (Shyamsunder Kumawat)

Abstract

This research investigates a fractional-order mathematical model for analyzing the dynamics of Monkeypox (Mpox) disease using the Caputo-Fabrizio derivative. The model incorporates both human and rodent populations, aiming to elucidate the disease's transmission mechanics, which is demonstrated to be more effective than integer-order models in capturing the complex nature of disease spread. The study determines the fundamental reproduction number (R_0) while assessing the existence and uniqueness of the solutions. Numerical simulations are conducted to validate the model using Adams-Bashforth technique and illustrate the influence of different factors on the progression of the disease. The findings shed light on Mpox control and prevention, emphasizing the importance of fractional calculus in epidemiological modeling.

Keywords: Adams-Bashforth technique; Caputo-Fabrizio derivative; existence and uniqueness; fixed point theorem; monkeypox virus

AMS 2020 Classification: 26A33; 92B05; 92D30; 92C50

1 Introduction

Monkeypox (Mpox) is a viral zoonotic disease that is transmitted between animals and humans, caused by the Mpox virus. This infection mostly occurs in Central and West Africa. Mpox became a significant orthopoxvirus for human health in 1980, after the eradication of smallpox infection. The first occurrence of this virus outside African nations was documented in 2003 in the United States. Afterwards, several instances of Mpox infection were recorded in countries across Africa and Europe [1]. In May 2022, the presence of the pathogen was verified in other nonendemic regions. The World Health Organization (WHO) received reports of about 3413 confirmed cases

and 1 fatality case from 50 countries/territories. Mpox is transmitted zoonotically from animals to humans [2]. Typically, the hosts in animals include a variety of rodents and non-human primates. The transmission of the virus may occur via interpersonal contact, particularly by droplets emitted during conversation, respiration, or sneezing. Additionally, it may be transferred by sexual contact with an individual who is contagious. Mpox may potentially be transmitted via the environment [3]. Wild animals, such as African rats and monkeys, are the primary sources of viral transmission to humans. Nevertheless, there is a high occurrence of human-to-human transmissions in the majority of the documented instances. Spreading diseases from animals to humans can occur through various mechanisms, including bites or scuffs the handling and consumption of bush meat, direct contact with body fluids, or the ingestion of food contaminated by rodents. The illness may be transmitted by direct contact with lesions and body fluids of infected individuals. Smallpox vaccination, antivirals, and vaccine immune globulin may serve as alternatives for preventing the transmission of Mpox. However, there is presently no established and reliable therapy for Mpox virus infection [4]. Mathematical models are crucial and have been widely used to examine the dynamics and provide effective ways to eliminate infectious illnesses from society [5, 6]. Those frameworks analyze quantitative aspects of the circumstance. Several epidemiological characteristics of Mpox infection are currently being studied [7, 8]. Ongoing research is being conducted to further investigate the transmission and treatment of this virus. Venkatesh et al. [9] established numerical method using new time fractional model for the Mpox. Also, Manivel et al. [10] developed a fractional mathematical modeling in humans and rodents for the Mpox disease. The numerical simulation indicates that individuals' immunological state has a significant role in their recovery process after orthopoxvirus infection. Several mathematical models [11] have been examined to enhance comprehension of the transmission dynamics and various strategies for managing endemic diseases.

The fractional modeling works synthesizes advanced mathematical modeling approaches to address epidemiological challenges by integrating key concepts from fractional-order models and stability analysis [12]. A mathematical model of mobility-related infection and vaccination is extended to consider the dynamics of SARS-CoV-2 through a Fractional SIQVR framework, emphasizing the role of fractional derivatives in capturing memory effects and complex dynamics [13]. Simultaneously, insights from a fractional-order model designed to analyze stability and propose sterilization strategies for the habitat of stray dogs are leveraged to develop holistic and adaptive intervention strategies [14]. Meanwhile, the SIR model with constrained medical resources and time delay examines the dynamics of healthcare system capacity and the impact of delayed interventions on disease progression [15]. This unified approach underscores the utility of fractional-order systems in understanding infection dynamics, vaccination impact, and the stability of populations, offering innovative solutions to pressing public health issues.

The primary motivation for this study arises from the increasing prevalence of Mpox infections outside traditionally endemic regions, underscoring the need for advanced mathematical tools to understand and predict the dynamics of its spread. Unlike classical integer-order models, fractional-order models can capture the memory effects and complex dynamics intrinsic to biological processes. This unique advantage provides a more accurate representation of Mpox's epidemiological patterns, which is crucial for effective disease control and prevention.

To enhance comprehension of the dynamics of Mpox, [16] formulated a mathematical model. The results indicate that Mpox may be effectively managed and eliminated by using vaccination strategies, even in regions where the disease is moderately prevalent. However, vaccination alone is insufficient to completely eliminate Mpox in a population that is already totally endemic [17]. In addition, the research conducted by [18] found that the recommended treatments resulted to the eradication of infected individuals in both human and non-human primate populations over the

study period, as shown by numerical simulations done on the model. Scientists and engineers from several fields have lately shown interest in using fractional differential equations for mathematical modeling, especially in the field of epidemiology. The memory effect is a fascinating characteristic of fractional-order framework that is absent in classical differential equations because of the diverse features of equations with fractions.

All Mpox transmission models currently in use solely account for transfer from animals to humans. There have been recent reports of transfer from humans to rodents. Based on the recent facts, in this paper, we develop the Mpox transmission model with animal-to-human transmission of infection. The aim of this research is to examine the spread and management of Mpox in the population by employing a classical and fractional-order model. Additionally, the study aims to examine the impact of the memory index or fractional order element on the dynamics of Mpox disease and determine whether it can be utilized as a control parameter.

The subsequent sections of the paper are structured as follows: [Section 2](#) discusses model formulations and analyses of the Mpox model. Findings on the existence and uniqueness of the model variable are elaborated in [Section 3](#). [Section 4](#) delineates the equilibrium and reproduction number with the parameters affecting R_0 . [Section 5](#) illustrates a numerical technique using the Adams-Bashforth method. [Section 6](#) includes the quantitative simulations and discussions pertaining to the model. [Section 7](#) presents a succinct conclusion.

Preliminaries

This section presents the essential foundational materials concerning fractional order operators.

Definition 1 [19] *The fractional derivative in the Caputo-Fabrizio (CF) sense for the function $H \in M^1(a, b)$, $b > a$, $\delta \in [0, 1]$ is characterized as*

$$D_t^\delta \{H(t)\} = \frac{M(\delta)}{1-\delta} \int_a^t H'(s) \exp\left(-\frac{\delta(t-s)}{1-\delta}\right) ds. \quad (1)$$

$M(\delta)$ is the normalized function that meets the criteria $M(0) = M(1) = 1$ [19]. In the scenario where $H \notin M^1(a, b)$ the aforementioned CF derivative can be articulated as

$$D_t^\delta \{H(t)\} = \frac{\delta M(\delta)}{1-\delta} \int_a^t (H(t) - H(s)) \exp\left(-\frac{\delta(t-s)}{1-\delta}\right) ds. \quad (2)$$

Remark 1 If $\alpha = \frac{1-\delta}{\delta} \in [0, \infty)$, $\delta = \frac{1}{1+\alpha} \in [0, 1]$, then Eq. (2) this can be written:

$$D_t^\alpha \{H(t)\} = \frac{N\alpha}{\delta} \int_a^t H'(s) \exp\left[-\frac{t-s}{\alpha}\right] ds, N(0) = N(\infty) = 1. \quad (3)$$

Moreover,

$$\lim_{\alpha \rightarrow 0} \frac{1}{\alpha} \exp\left[-\frac{t-s}{\alpha}\right] = \tau(s-t).$$

The integral that is related to the CF derivative is described as follows [20]. The initial function $H(t)$ is assumed to satisfy the regularity conditions required for the application of the CF derivative. Specifically, $H(t)$ is considered to be a member of $M_1(a, b)$, ensuring it possesses the necessary smoothness and

boundedness over the interval of interest. Moreover, the model presumes that the initial conditions $H(t_0) = H_0$ align with the physical or epidemiological study.

Definition 2 While $t > 0$ and $M(\delta)$ indicates the normalization function, In such a way that $M(1) = 0 = M(0)$. It is presumed that $0 < \delta < 1$ and $H(t)$, is dependent on t , then the Riemann-Liouville fractional crucial of order δ is characterized as

$${}^{RL}I_{0,t}^{\delta}\{H(t)\} = \frac{1}{\Gamma(\delta)} \int_0^t (t-s)^{\delta-1} H(s) ds,$$

the Caputo-Fabrizio integral of order δ is expressed as

$${}^{CF}I_{0,t}^{\delta}\{H(t)\} = \frac{2(1-\delta)H(t)}{(2-\delta)M(\delta)} + \frac{2\delta}{(2-\delta)M(\delta)} \int_0^t H(s) ds, \quad (4)$$

where $t \geq 0$.

2 Mpox model formulation

In order to create the model, the complete human population N_m divided into six distinct categories, namely susceptible S_m , exposed E_m , infected I_m , asymptotically-ill A_m , vaccinated V_m , and recovered humans R_m . Likewise, the total rodent population is N_a . It is further separated into three distinct categories, namely susceptible S_a , exposed E_a , and infected rodent I_a groups.

The initiation of the susceptible human class occurs through two mechanisms: either by birth or through the immigration of susceptible individuals at a specified rate Π_m and from the vaccinated population following the decline of the induced immunity at a specified rate τ . The natural death rate declines throughout human classes μ_1 . The group of individuals susceptible to infection is diminished as a result of vaccination at the specified rate α_m and as a result of the interaction with infected humans and animals. Consequently, the individuals who are susceptible transition to the exposed category at the rate of infection force λ_1 depicts as: $\lambda_1 = \left(\frac{\beta_1 I_m + \beta_2 I_a + \beta_3 A_m}{N_m} \right)$.

The interaction terms in the model are derived from fundamental epidemiological principles. These terms capture the probabilistic nature of contacts leading to disease transmission. The force of infection for the human population λ_1 includes $\frac{\beta_1 I_m + \beta_2 I_a + \beta_3 A_m}{N_m}$, where the numerators represent interactions between susceptible and infectious individuals across compartments, scaled by their respective contact rates. These interactions reflect real-world dynamics, where direct or indirect contacts between infected and susceptible humans lead to new exposures.

The choice to multiply these variables ensures that the rate of new infections is proportional to the number of infectious individuals, their contact rates, and the availability of susceptible individuals. Exposed individuals transition to either asymptomatic or symptomatic infectious states ($E_m \rightarrow A_m, I_m$) based on progression rates ($k(1-\rho)$ and $k\rho$ respectively). It is emphasized that the interactions in the model occur via rates that represent indirect effects (e.g., disease transmission or recovery) rather than direct inter-compartmental mixing. This separation ensures that the model accurately depicts real-world disease transmission while maintaining mathematical and conceptual simplicity. The parameters β_1, β_2 , and β_3 are the effective contact rates. The group of susceptible animals, which includes primates or rodents, is established through the incorporation of newly enlisted animals Π_a . The number of individuals in the susceptible class decreases as a result of two key factors: The phrase $\lambda_2 = \frac{\beta_4 I_a}{N_a}$, it considers the connection among vulnerable animals (primates or rats) and infected ones, as well as the natural mortality rate μ_2 .

Consequently, the system illustrating the spreading processes of Mpox in both populations is as described below:

$$\begin{aligned}
 \frac{dS_m}{dt} &= \Pi_m - \lambda_1 S_m - (\mu_1 + \alpha_m) S_m + \tau V_m, \\
 \frac{dE_m}{dt} &= \lambda_1 S_m - (k + \mu_1) E_m, \\
 \frac{dA_m}{dt} &= k(1 - \rho) E_m - (\gamma_1 + \mu_1 + \eta_1) A_m, \\
 \frac{dI_m}{dt} &= k\rho E_m - (\gamma_2 + \mu_1 + \eta_2) I_m, \\
 \frac{dV_m}{dt} &= \alpha_m S_m - (\tau + \mu_1) V_m, \\
 \frac{dR_m}{dt} &= \gamma_1 A_m + \gamma_2 I_m - \mu_1 R_m, \\
 \frac{dS_a}{dt} &= \Pi_a - \lambda_2 S_a - \mu_2 S_a, \\
 \frac{dE_a}{dt} &= \lambda_2 S_a - (\pi + \mu_2) E_a, \\
 \frac{dI_a}{dt} &= \pi E_a - (\mu_2 + \eta_3) I_a.
 \end{aligned} \tag{5}$$

The flowchart of the problem explained in system (5) is given in the following Figure 1.

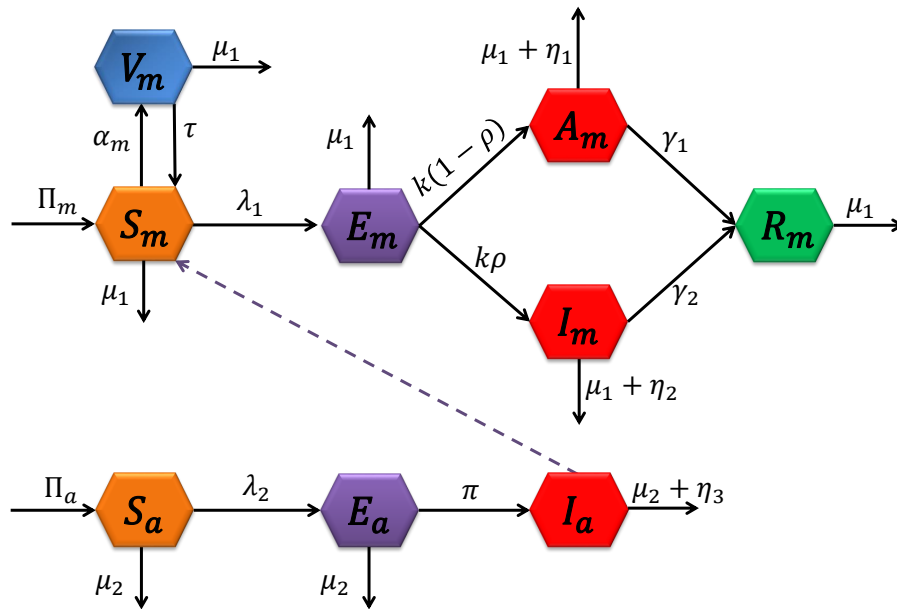


Figure 1. Graphical representation of Mpox model

The Caputo fractional derivative was used for this investigation because it accommodates initial conditions articulated in integer-order derivatives, which is consistent with the majority of physical and epidemiological issues. In contrast to Riemann-Liouville derivatives, the Caputo derivative

permits the direct integration of real-world initial conditions, hence enhancing the intuitive and practical use of fractional calculus in modeling infectious disease dynamics. The Caputo operator is well suited for numerical approaches, guaranteeing stability and precision in simulations, which is essential for accurately portraying the intricate memory effects of Mpox transmission. The memory effects, characterized by the non-local properties of the Caputo derivative, provide a more thorough comprehension of disease dynamics compared to integer-order models. In addition, unlike the CF derivative, which emphasizes exponential decay, the classical Caputo derivative provides versatility in characterizing long-range temporal interactions inherent to epidemiological phenomena. Replacing the integer order model (5) with non-integer order in CF operator with each differential equation's dimension maintained as stated:

$$\begin{aligned}
 {}^{CF}D_{0,t}^{\delta}(S_m(t)) &= \Pi_m - \lambda_1 S_m - (\mu_1 + \alpha_m) S_m + \tau V_m, \\
 {}^{CF}D_{0,t}^{\delta}(E_m(t)) &= \lambda_1 S_m - (k + \mu_1) E_m, \\
 {}^{CF}D_{0,t}^{\delta}(A_m(t)) &= k(1 - \rho) E_m - (\gamma_1 + \mu_1 + \eta_1) A_m, \\
 {}^{CF}D_{0,t}^{\delta}(I_m(t)) &= k\rho E_m - (\gamma_2 + \mu_1 + \eta_2) I_m, \\
 {}^{CF}D_{0,t}^{\delta}(V_m(t)) &= \alpha_m S_m - (\tau + \mu_1) V_m, \\
 {}^{CF}D_{0,t}^{\delta}(R_m(t)) &= \gamma_1 A_m + \gamma_2 I_m - \mu_1 R_m, \\
 {}^{CF}D_{0,t}^{\delta}(S_a(t)) &= \Pi_a - \lambda_2 S_a - \mu_2 S_a, \\
 {}^{CF}D_{0,t}^{\delta}(E_a(t)) &= \lambda_2 S_a - (\pi + \mu_2) E_a, \\
 {}^{CF}D_{0,t}^{\delta}(I_a(t)) &= \pi E_a - (\mu_2 + \eta_3) I_a,
 \end{aligned} \tag{6}$$

with regard to the initial conditions involved in system (6) are $S_m(0) = S_{m0}$, $E_m(0) = E_{m0}$, $A_m(0) = A_{m0}$, $I_m(0) = I_{m0}$, $V_m(0) = V_{m0}$, $R_m(0) = R_{m0}$, $S_a(0) = S_{a0}$, $E_a(0) = E_{a0}$, $I_a(0) = I_{a0}$.

3 Model analysis in the fractional case

We will examine fundamental mathematical elements of the Mpox compartmental epidemiological model in fractional form as outlined in (6).

Existence and uniqueness

This section will demonstrate the outcome of the fractional-order model (6) through an analysis of fixed point hypothesis. This is achieved by reformulating the fractional-order differential equations as integral equations and verifying the Lipschitz conditions for all model kernels. We will additionally demonstrate the uniqueness of the remedy. To achieve this, the initial step involves converting the proposed fractional order system into a corresponding integral equation structure as follows:

$$\begin{aligned}
 S_m(t) - S_m(0) &= {}^{CF}I_{0,t}^{\delta}\{\Pi_m - \lambda_1 S_m - (\mu_1 + \alpha_m) S_m + \tau V_m\}, \\
 E_m(t) - E_m(0) &= {}^{CF}I_{0,t}^{\delta}\{\lambda_1 S_m - (k + \mu_1) E_m\}, \\
 A_m(t) - A_m(0) &= {}^{CF}I_{0,t}^{\delta}\{k(1 - \rho) E_m - (\gamma_1 + \mu_1 + \eta_1) A_m\}, \\
 I_m(t) - I_m(0) &= {}^{CF}I_{0,t}^{\delta}\{k\rho E_m - (\gamma_2 + \mu_1 + \eta_2) I_m\}, \\
 V_m(t) - V_m(0) &= {}^{CF}I_{0,t}^{\delta}\{\alpha_m S_m - (\tau + \mu_1) V_m\}, \\
 R_m(t) - R_m(0) &= {}^{CF}I_{0,t}^{\delta}\{\gamma_1 A_m + \gamma_2 I_m - \mu_1 R_m\}, \\
 S_a(t) - S_a(0) &= {}^{CF}I_{0,t}^{\delta}\{\Pi_a - \lambda_2 S_a - \mu_2 S_a\},
 \end{aligned} \tag{7}$$

$$\begin{aligned} E_a(t) - E_a(0) &= {}^{CF}I_{0,t}^\delta \{\lambda_2 S_a - (\pi + \mu_2) E_a\}, \\ I_a(t) - I_a(0) &= {}^{CF}I_{0,t}^\delta \{\pi E_a - (\mu_2 + \eta_3) I_a\}. \end{aligned}$$

Through the implementation of CF fractional order integrating [20], one can acquire

$$\begin{aligned} S_m(t) - S_m(0) &= \frac{2(1-\delta)}{(2-\delta)M(\delta)} J_1(t, S_m) + \frac{2\delta}{(2-\delta)M(\delta)} \int_0^t J_1(x, S_m) dx, \\ E_m(t) - E_m(0) &= \frac{2(1-\delta)}{(2-\delta)M(\delta)} J_2(t, E_m) + \frac{2\delta}{(2-\delta)M(\delta)} \int_0^t J_2(x, E_m) dx, \\ A_m(t) - A_m(0) &= \frac{2(1-\delta)}{(2-\delta)M(\delta)} J_3(t, A_m) + \frac{2\delta}{(2-\delta)M(\delta)} \int_0^t J_3(x, A_m) dx, \\ I_m(t) - I_m(0) &= \frac{2(1-\delta)}{(2-\delta)M(\delta)} J_4(t, I_m) + \frac{2\delta}{(2-\delta)M(\delta)} \int_0^t J_4(x, I_m) dx, \\ V_m(t) - V_m(0) &= \frac{2(1-\delta)}{(2-\delta)M(\delta)} J_5(t, V_m) + \frac{2\delta}{(2-\delta)M(\delta)} \int_0^t J_5(x, V_m) dx, \\ R_m(t) - R_m(0) &= \frac{2(1-\delta)}{(2-\delta)M(\delta)} J_6(t, R_m) + \frac{2\delta}{(2-\delta)M(\delta)} \int_0^t J_6(x, R_m) dx, \\ S_a(t) - S_a(0) &= \frac{2(1-\delta)}{(2-\delta)M(\delta)} J_7(t, S_a) + \frac{2\delta}{(2-\delta)M(\delta)} \int_0^t J_7(x, S_a) dx, \\ E_a(t) - E_a(0) &= \frac{2(1-\delta)}{(2-\delta)M(\delta)} J_8(t, E_a) + \frac{2\delta}{(2-\delta)M(\delta)} \int_0^t J_8(x, E_a) dx, \\ I_a(t) - I_a(0) &= \frac{2(1-\delta)}{(2-\delta)M(\delta)} J_9(t, I_a) + \frac{2\delta}{(2-\delta)M(\delta)} \int_0^t J_9(x, I_a) dx. \end{aligned}$$

We assume kernels as determined by

$$\begin{aligned} J_1(S_m(t), t) &= \Pi_m - \lambda_1 S_m - (\mu_1 + \alpha_m) S_m + \tau V_m, \\ J_2(E_m(t), t) &= \lambda_1 S_m - (k + \mu_1) E_m, \\ J_3(A_m(t), t) &= k(1 - \rho) E_m - (\gamma_1 + \mu_1 + \eta_1) A_m, \\ J_4(I_m(t), t) &= k\rho E_m - (\gamma_2 + \mu_1 + \eta_2) I_m, \\ J_5(V_m(t), t) &= \alpha_m S_m - (\tau + \mu_1) V_m, \\ J_6(R_m(t), t) &= \gamma_1 A_m + \gamma_2 I_m - \mu_1 R_m, \\ J_7(S_a(t), t) &= \Pi_a - \lambda_2 S_a - \mu_2 S_a, \\ J_8(E_a(t), t) &= \lambda_2 S_a - (\pi + \mu_2) E_a, \\ J_9(I_a(t), t) &= \pi E_a - (\mu_2 + \eta_3) I_a. \end{aligned} \tag{8}$$

Theorem 1 The kernels $J_1, J_2, J_3, J_4, J_5, J_6, J_7, J_8$, and J_9 meet the Lipschitz criteria.

Proof Let us imagine that S_m and S_{m_1} , E_m and E_{m_1} , A_m and A_{m_1} , I_m and I_{m_1} , V_m and V_{m_1} , R_m and R_{m_1} , S_a and S_{a_1} , E_a and E_{a_1} , I_a and I_{a_1} , represents the two functions corresponding to the

aforementioned kernels $J_1, J_2, J_3, J_4, J_5, J_6, J_7, J_8$, and J_9 . Thus, we set up the subsequent system

$$\begin{aligned}
J_1(S_m(t), t) - J_1(S_{m_1}(t), t) &= -\lambda_1(S_m(t) - S_{m_1}(t)) - (\mu_1 + \alpha_m)(S_m(t) - S_{m_1}(t)) \\
&\quad + \tau(V_m(t) - V_{m_1}(t)), \\
J_2(E_m(t), t) - J_2(E_{m_1}(t), t) &= \lambda_1(S_m(t) - S_{m_1}(t)) - (k + \mu_1)(E_m(t) - E_{m_1}(t)), \\
J_3(A_m(t), t) - J_3(A_{m_1}(t), t) &= k(1 - \rho)(E_m(t) - E_{m_1}(t)) - (\gamma_1 + \mu_1 + \eta_1)(A_m(t) - A_{m_1}(t)), \\
J_4(I_m(t), t) - J_4(I_{m_1}(t), t) &= k\rho(E_m(t) - E_{m_1}(t)) - (\gamma_2 + \mu_1 + \eta_2)(I_m(t) - I_{m_1}(t)), \\
J_5(V_m(t), t) - J_5(V_{m_1}(t), t) &= \alpha_m(S_m(t) - S_{m_1}(t)) - (\tau + \mu_1)(V_m(t) - V_{m_1}(t)), \\
J_6(R_m(t), t) - J_6(R_{m_1}(t), t) &= \gamma_1(A_m(t) - A_{m_1}(t)) + \gamma_2(I_m(t) - I_{m_1}(t)) \\
&\quad - \mu_1(R_m(t) - R_{m_1}(t)), \\
J_7(S_a(t), t) - J_7(S_{a_1}(t), t) &= -(\lambda_2 + \mu_2)(S_a(t) - S_{a_1}(t)), \\
J_8(E_a(t), t) - J_8(E_{a_1}(t), t) &= \lambda_2 S_a(t) - S_{a_1}(t) - (\pi + \mu_2)(E_a(t) - E_{a_1}(t)), \\
J_9(I_a(t), t) - J_9(I_{a_1}(t), t) &= \pi(E_a(t) - E_{a_1}(t)) - (\mu_2 + \eta_3)(I_a(t) - I_{a_1}(t)).
\end{aligned}$$

By applying Cauchy's inequality to the aforementioned system, it is possible to derive

$$\begin{aligned}
\|J_1(S_m(t), t) - J_1(S_{m_1}(t), t)\| &= \|-\lambda_1(S_m(t) - S_{m_1}(t)) - (\mu_1 + \alpha_m)(S_m(t) - S_{m_1}(t)) \\
&\quad + \tau(V_m(t) - V_{m_1}(t))\| \\
&\leq \|\lambda_1 + \mu_1 + \alpha_m\| \|S_m(t) - S_{m_1}(t)\|, \\
\|J_2(E_m(t), t) - J_2(E_{m_1}(t), t)\| &= \|\lambda_1(S_m(t) - S_{m_1}(t)) - (k + \mu_1)(E_m(t) - E_{m_1}(t))\| \\
&\leq \|\lambda_1 + k + \mu_1\| \|E_m(t) - E_{m_1}(t)\|, \\
\|J_3(A_m(t), t) - J_3(A_{m_1}(t), t)\| &= \|k(1 - \rho)(E_m(t) - E_{m_1}(t)) - (\gamma_1 + \mu_1 + \eta_1)(A_m(t) - A_{m_1}(t))\| \\
&\leq \|k(1 - \rho) + \gamma_1 + \mu_1 + \eta_1\| \|A_m(t) - A_{m_1}(t)\|, \\
\|J_4(I_m(t), t) - J_4(I_{m_1}(t), t)\| &= \|k\rho(E_m(t) - E_{m_1}(t)) - (\gamma_2 + \mu_1 + \eta_2)(I_m(t) - I_{m_1}(t))\| \\
&\leq \|k\rho + \gamma_2 + \mu_1 + \eta_2\| \|I_m(t) - I_{m_1}(t)\|, \\
\|J_5(V_m(t), t) - J_5(V_{m_1}(t), t)\| &= \|\alpha_m(S_m(t) - S_{m_1}(t)) - (\tau + \mu_1)(V_m(t) - V_{m_1}(t))\| \\
&\leq \|\alpha_m + \tau + \mu_1\| \|V_m(t) - V_{m_1}(t)\|, \\
\|J_6(R_m(t), t) - J_6(R_{m_1}(t), t)\| &= \|\gamma_1(A_m(t) - A_{m_1}(t)) + \gamma_2(I_m(t) - I_{m_1}(t)) \\
&\quad - \mu_1(R_m(t) - R_{m_1}(t))\| \\
&\leq \|\gamma_1 + \gamma_2 + \mu_1\| \|R_m(t) - R_{m_1}(t)\|, \\
\|J_7(S_a(t), t) - J_7(S_{a_1}(t), t)\| &= \|-(\lambda_2 + \mu_2)(S_a(t) - S_{a_1}(t))\| \\
&\leq \|\lambda_2 + \mu_2\| \|S_a(t) - S_{a_1}(t)\|, \\
\|J_8(E_a(t), t) - J_8(E_{a_1}(t), t)\| &= \|\lambda_2 S_a(t) - S_{a_1}(t) - (\pi + \mu_2)(E_a(t) - E_{a_1}(t))\| \\
&\leq \|\lambda_2 + \pi + \mu_2\| \|E_a(t) - E_{a_1}(t)\|, \\
\|J_9(I_a(t), t) - J_9(I_{a_1}(t), t)\| &= \|\pi(E_a(t) - E_{a_1}(t)) - (\mu_2 + \eta_3)(I_a(t) - I_{a_1}(t))\| \\
&\leq \|\pi + \mu_2 + \eta_3\| \|I_a(t) - I_{a_1}(t)\|.
\end{aligned}$$

Employing the definition of the CF fractional integral, recursively, one may obtain

$$\begin{aligned}
S_m(t) &= \frac{2(1-\delta)J_1(S_{m_{n-1}}(t), t)}{(2-\delta)M(\delta)} + \frac{2\delta}{(2-\delta)M(\delta)} \int_0^t J_1(S_{m_{n-1}}(s), s) ds, \\
E_m(t) &= \frac{2(1-\delta)J_2(E_{m_{n-1}}(t), t)}{(2-\delta)M(\delta)} + \frac{2\delta}{(2-\delta)M(\delta)} \int_0^t J_2(E_{m_{n-1}}(s), s) ds, \\
A_m(t) &= \frac{2(1-\delta)J_3(A_{m_{n-1}}(t), t)}{(2-\delta)M(\delta)} + \frac{2\delta}{(2-\delta)M(\delta)} \int_0^t J_3(A_{m_{n-1}}(s), s) ds, \\
I_m(t) &= \frac{2(1-\delta)J_4(I_{m_{n-1}}(t), t)}{(2-\delta)M(\delta)} + \frac{2\delta}{(2-\delta)M(\delta)} \int_0^t J_4(I_{m_{n-1}}(s), s) ds, \\
V_m(t) &= \frac{2(1-\delta)J_5(V_{m_{n-1}}(t), t)}{(2-\delta)M(\delta)} + \frac{2\delta}{(2-\delta)M(\delta)} \int_0^t J_5(V_{m_{n-1}}(s), s) ds, \\
R_m(t) &= \frac{2(1-\delta)J_6(R_{m_{n-1}}(t), t)}{(2-\delta)M(\delta)} + \frac{2\delta}{(2-\delta)M(\delta)} \int_0^t J_6(R_{m_{n-1}}(s), s) ds, \\
S_a(t) &= \frac{2(1-\delta)J_7(S_{a_{n-1}}(t), t)}{(2-\delta)M(\delta)} + \frac{2\delta}{(2-\delta)M(\delta)} \int_0^t J_7(S_{a_{n-1}}(s), s) ds, \\
E_a(t) &= \frac{2(1-\delta)J_8(E_{a_{n-1}}(t), t)}{(2-\delta)M(\delta)} + \frac{2\delta}{(2-\delta)M(\delta)} \int_0^t J_8(E_{a_{n-1}}(s), s) ds, \\
I_a(t) &= \frac{2(1-\delta)J_9(I_{a_{n-1}}(t), t)}{(2-\delta)M(\delta)} + \frac{2\delta}{(2-\delta)M(\delta)} \int_0^t J_9(I_{a_{n-1}}(s), s) ds.
\end{aligned} \tag{9}$$

The utilization of norms the concept of majorizing indicates that the variance among successive terms suggests

$$\begin{aligned}
\|\mathcal{K}_n(t)\| &= \|S_{m_n}(t) - S_{m_{1,n-1}}\| \leq \frac{2(1-\delta)}{(2-\delta)M(\delta)} \|J_1(S_{m_{n-1}}(t), t) - J_1(S_{m_{1,n-2}}(t), t)\| \\
&\quad + \frac{2\delta}{(2-\delta)M(\delta)} \left\| \int_0^t [J_1(S_{m_{n-1}}(s), s) - J_1(S_{m_{1,n-2}}(s), s)] ds \right\|,
\end{aligned}$$

$$\begin{aligned}
\|\mathcal{L}_n(t)\| &= \|E_{m_n}(t) - E_{m_{1,n-1}}\| \leq \frac{2(1-\delta)}{(2-\delta)M(\delta)} \|J_2(E_{m_{n-1}}(t), t) - J_2(E_{m_{1,n-2}}(t), t)\| \\
&\quad + \frac{2\delta}{(2-\delta)M(\delta)} \left\| \int_0^t [J_2(E_{m_{n-1}}(s), s) - J_2(E_{m_{1,n-2}}(s), s)] ds \right\|,
\end{aligned}$$

$$\begin{aligned}
\|\mathcal{M}_n(t)\| &= \|A_{m_n}(t) - A_{m_{1,n-1}}\| \leq \frac{2(1-\delta)}{(2-\delta)M(\delta)} \|J_3(A_{m_{n-1}}(t), t) - J_3(A_{m_{1,n-2}}(t), t)\| \\
&\quad + \frac{2\delta}{(2-\delta)M(\delta)} \left\| \int_0^t [J_3(A_{m_{n-1}}(s), s) - J_3(A_{m_{1,n-2}}(s), s)] ds \right\|,
\end{aligned}$$

$$\begin{aligned}\|\mathcal{N}_n(t)\| &= \|I_{m_n}(t) - I_{m_{1,n-1}}\| \leq \frac{2(1-\delta)}{(2-\delta)M(\delta)} \|J_4(I_{m_{n-1}}(t), t) - J_4(I_{m_{1,n-2}}(t), t)\| \\ &\quad + \frac{2\delta}{(2-\delta)M(\delta)} \left\| \int_0^t [J_4(I_{m_{n-1}}(s), s) - J_4(I_{m_{1,n-2}}(s), s)] ds \right\|,\end{aligned}$$

$$\begin{aligned}\|\mathcal{O}_n(t)\| &= \|V_{m_n}(t) - V_{m_{1,n-1}}\| \leq \frac{2(1-\delta)}{(2-\delta)M(\delta)} \|J_5(V_{m_{n-1}}(t), t) - J_5(V_{m_{1,n-2}}(t), t)\| \\ &\quad + \frac{2\delta}{(2-\delta)M(\delta)} \left\| \int_0^t [J_5(V_{m_{n-1}}(s), s) - J_5(V_{m_{1,n-2}}(s), s)] ds \right\|,\end{aligned}$$

$$\begin{aligned}\|\mathcal{P}_n(t)\| &= \|R_{m_n}(t) - R_{m_{1,n-1}}\| \leq \frac{2(1-\delta)}{(2-\delta)M(\delta)} \|J_6(R_{m_{n-1}}(t), t) - J_6(R_{m_{1,n-2}}(t), t)\| \\ &\quad + \frac{2\delta}{(2-\delta)M(\delta)} \left\| \int_0^t [J_6(R_{m_{n-1}}(s), s) - J_6(R_{m_{1,n-2}}(s), s)] ds \right\|,\end{aligned}$$

$$\begin{aligned}\|\mathcal{X}_n(t)\| &= \|S_{a_n}(t) - S_{a_{1,n-1}}\| \leq \frac{2(1-\delta)}{(2-\delta)M(\delta)} \|J_7(S_{a_{n-1}}(t), t) - J_7(S_{a_{1,n-2}}(t), t)\| \\ &\quad + \frac{2\delta}{(2-\delta)M(\delta)} \left\| \int_0^t [J_7(S_{a_{n-1}}(s), s) - J_7(S_{a_{1,n-2}}(s), s)] ds \right\|,\end{aligned}$$

$$\begin{aligned}\|\mathcal{Y}_n(t)\| &= \|E_{a_n}(t) - E_{a_{1,n-1}}\| \leq \frac{2(1-\delta)}{(2-\delta)M(\delta)} \|J_8(E_{a_{n-1}}(t), t) - J_8(E_{a_{1,n-2}}(t), t)\| \\ &\quad + \frac{2\delta}{(2-\delta)M(\delta)} \left\| \int_0^t [J_8(S_{a_{n-1}}(s), s) - J_8(E_{a_{1,n-2}}(s), s)] ds \right\|,\end{aligned}$$

$$\begin{aligned}\|\mathcal{Z}_n(t)\| &= \|I_{a_n}(t) - I_{a_{1,n-1}}\| \leq \frac{2(1-\delta)}{(2-\delta)M(\delta)} \|J_9(I_{a_{n-1}}(t), t) - J_9(I_{a_{1,n-2}}(t), t)\| \\ &\quad + \frac{2\delta}{(2-\delta)M(\delta)} \left\| \int_0^t [J_9(I_{a_{n-1}}(s), s) - J_9(I_{a_{1,n-2}}(s), s)] ds \right\|,\end{aligned}$$

where

$$\begin{aligned}\sum_{i=0}^{\infty} \mathcal{K}_i(t) &= S_{m_n}(t), \quad \sum_{i=0}^{\infty} \mathcal{L}_i(t) = E_{m_n}(t), \quad \sum_{i=0}^{\infty} \mathcal{M}_i(t) = A_{m_n}(t), \quad \sum_{i=0}^{\infty} \mathcal{N}_i(t) = I_{m_n}(t), \\ \sum_{i=0}^{\infty} \mathcal{O}_i(t) &= V_{h_n}(t), \quad \sum_{i=0}^{\infty} \mathcal{P}_i(t) = R_{m_n}(t), \quad \sum_{i=0}^{\infty} \mathcal{X}_i(t) = S_{a_n}(t), \quad \sum_{i=0}^{\infty} \mathcal{Y}_i(t) = E_{a_n}(t), \\ \sum_{i=0}^{\infty} \mathcal{Z}_i(t) &= I_{a_n}(t).\end{aligned}\tag{10}$$

Moreover, the kernels J_1, \dots, J_9 fulfill the Lipschitz condition, allowing one to express

$$\begin{aligned} \|\mathcal{K}_n(t)\| &= \|S_{m_n}(t) - S_{m_{1,n-1}}\| \leq \frac{2(1-\delta)}{(2-\delta)M(\delta)} \xi_1 \|S_{m_{n-1}}(t) - S_{m_{1,n-2}}(t)\| \\ &\quad + \frac{2\delta}{(2-\delta)M(\delta)} \xi_2 \left\| \int_0^t S_{m_{n-1}}(s) - S_{m_{1,n-2}}(s) ds \right\|, \end{aligned}$$

$$\begin{aligned} \|\mathcal{L}_n(t)\| &= \|E_{m_n}(t) - E_{m_{1,n-1}}\| \leq \frac{2(1-\delta)}{(2-\delta)M(\delta)} \xi_3 \|E_{m_{n-1}}(t) - E_{m_{1,n-2}}(t)\| \\ &\quad + \frac{2\delta}{(2-\delta)M(\delta)} \xi_4 \left\| \int_0^t E_{m_{n-1}}(s) - E_{m_{1,n-2}}(s) ds \right\|, \end{aligned}$$

$$\begin{aligned} \|\mathcal{M}_n(t)\| &= \|A_{m_n}(t) - A_{m_{1,n-1}}\| \leq \frac{2(1-\delta)}{(2-\delta)M(\delta)} \xi_5 \|A_{m_{n-1}}(t) - A_{m_{1,n-2}}(t)\| \\ &\quad + \frac{2\delta}{(2-\delta)M(\delta)} \xi_6 \left\| \int_0^t A_{m_{n-1}}(s) - A_{m_{1,n-2}}(s) ds \right\|, \end{aligned}$$

$$\begin{aligned} \|\mathcal{N}_n(t)\| &= \|I_{m_n}(t) - I_{m_{1,n-1}}\| \leq \frac{2(1-\delta)}{(2-\delta)M(\delta)} \xi_7 \|I_{m_{n-1}}(t) - I_{m_{1,n-2}}(t)\| \\ &\quad + \frac{2\delta}{(2-\delta)M(\delta)} \xi_8 \left\| \int_0^t I_{m_{n-1}}(s) - I_{m_{1,n-2}}(s) ds \right\|, \end{aligned}$$

$$\begin{aligned} \|\mathcal{O}_n(t)\| &= \|V_{m_n}(t) - V_{m_{1,n-1}}\| \leq \frac{2(1-\delta)}{(2-\delta)M(\delta)} \xi_9 \|V_{m_{n-1}}(t) - V_{m_{1,n-2}}(t)\| \\ &\quad + \frac{2\delta}{(2-\delta)M(\delta)} \xi_{10} \left\| \int_0^t V_{m_{n-1}}(s) - V_{m_{1,n-2}}(s) ds \right\|, \end{aligned}$$

$$\begin{aligned} \|\mathcal{P}_n(t)\| &= \|R_{m_n}(t) - R_{m_{1,n-1}}\| \leq \frac{2(1-\delta)}{(2-\delta)M(\delta)} \xi_{11} \|R_{m_{n-1}}(t) - R_{m_{1,n-2}}(t)\| \\ &\quad + \frac{2\delta}{(2-\delta)M(\delta)} \xi_{12} \left\| \int_0^t R_{m_{n-1}}(s) - R_{m_{1,n-2}}(s) ds \right\|, \end{aligned}$$

$$\begin{aligned} \|\mathcal{X}_n(t)\| &= \|S_{a_n}(t) - S_{a_{1,n-1}}\| \leq \frac{2(1-\delta)}{(2-\delta)M(\delta)} \xi_{13} \|S_{a_{n-1}}(t) - S_{a_{1,n-2}}(t)\| \\ &\quad + \frac{2\delta}{(2-\delta)M(\delta)} \xi_{14} \left\| \int_0^t S_{a_{n-1}}(s) - S_{a_{1,n-2}}(s) ds \right\|, \end{aligned}$$

$$\begin{aligned}\|\mathcal{Y}_n(t)\| &= \|E_{a_n}(t) - E_{a_{1,n-1}}\| \leq \frac{2(1-\delta)}{(2-\delta)M(\delta)}\xi_{15}\|E_{a_{n-1}}(t) - E_{a_{1,n-2}}(t)\| \\ &\quad + \frac{2\delta}{(2-\delta)M(\delta)}\xi_{16}\left\|\int_0^t E_{a_{n-1}}(s) - E_{a_{1,n-2}}(s)ds\right\|,\end{aligned}$$

$$\begin{aligned}\|\mathcal{Z}_n(t)\| &= \|I_{a_n}(t) - I_{a_{1,n-1}}\| \leq \frac{2(1-\delta)}{(2-\delta)M(\delta)}\xi_{17}\|I_{a_{n-1}}(t) - I_{a_{1,n-2}}(t)\| \\ &\quad + \frac{2\delta}{(2-\delta)M(\delta)}\xi_{18}\left\|\int_0^t I_{a_{n-1}}(s) - I_{a_{1,n-2}}(s)ds\right\|.\end{aligned}$$

Theorem 2 *The existence of the solution for the introduced fractional order model (6) is established based on the CF operator.*

Proof The utilization of Eq. (10) along with the implementation of a recursive scheme results in the subsequent system

$$\begin{aligned}\|\mathcal{K}_n(t)\| &\leq \|S_m(0)\| + \left\{\left(\frac{2\xi_1(1-\delta)}{M(\delta)(2-\delta)}\right)^n\right\} + \left\{\left(\frac{2\xi_2\delta t}{M(\delta)(2-\delta)}\right)^n\right\}, \\ \|\mathcal{L}_n(t)\| &\leq \|E_m(0)\| + \left\{\left(\frac{2\xi_3(1-\delta)}{M(\delta)(2-\delta)}\right)^n\right\} + \left\{\left(\frac{2\xi_4\delta t}{M(\delta)(2-\delta)}\right)^n\right\}, \\ \|\mathcal{M}_n(t)\| &\leq \|A_m(0)\| + \left\{\left(\frac{2\xi_5(1-\delta)}{M(\delta)(2-\delta)}\right)^n\right\} + \left\{\left(\frac{2\xi_6\delta t}{M(\delta)(2-\delta)}\right)^n\right\}, \\ \|\mathcal{N}_n(t)\| &\leq \|I_m(0)\| + \left\{\left(\frac{2\xi_7(1-\delta)}{M(\delta)(2-\delta)}\right)^n\right\} + \left\{\left(\frac{2\xi_8\delta t}{M(\delta)(2-\delta)}\right)^n\right\}, \\ \|\mathcal{O}_n(t)\| &\leq \|V_m(0)\| + \left\{\left(\frac{2\xi_9(1-\delta)}{M(\delta)(2-\delta)}\right)^n\right\} + \left\{\left(\frac{2\xi_{10}\delta t}{M(\delta)(2-\delta)}\right)^n\right\}, \\ \|\mathcal{P}_n(t)\| &\leq \|R_m(0)\| + \left\{\left(\frac{2\xi_{11}(1-\delta)}{M(\delta)(2-\delta)}\right)^n\right\} + \left\{\left(\frac{2\xi_{12}\delta t}{M(\delta)(2-\delta)}\right)^n\right\}, \\ \|\mathcal{X}_n(t)\| &\leq \|S_a(0)\| + \left\{\left(\frac{2\xi_{13}(1-\delta)}{M(\delta)(2-\delta)}\right)^n\right\} + \left\{\left(\frac{2\xi_{14}\delta t}{M(\delta)(2-\delta)}\right)^n\right\}, \\ \|\mathcal{Y}_n(t)\| &\leq \|E_a(0)\| + \left\{\left(\frac{2\xi_{15}(1-\delta)}{M(\delta)(2-\delta)}\right)^n\right\} + \left\{\left(\frac{2\xi_{16}\delta t}{M(\delta)(2-\delta)}\right)^n\right\}, \\ \|\mathcal{Z}_n(t)\| &\leq \|I_a(0)\| + \left\{\left(\frac{2\xi_{17}(1-\delta)}{M(\delta)(2-\delta)}\right)^n\right\} + \left\{\left(\frac{2\xi_{18}\delta t}{M(\delta)(2-\delta)}\right)^n\right\}.\end{aligned}\tag{11}$$

To examine whether the functions in Eq. (11) serve as solutions to the model (6), we will employ

the subsequent replacements

$$\begin{aligned} S_m(t) &= S_{m_n}(t) - Y_{1,n}(t), \quad E_m(t) = E_{m_n}(t) - Y_{2,n}(t), \quad A_m(t) = A_{m_n}(t) - Y_{3,n}(t), \\ I_m(t) &= I_{m_n}(t) - Y_{4,n}(t), \quad V_m(t) = V_{m_n}(t) - Y_{5,n}(t), \quad R_m(t) = R_{m_n}(t) - Y_{6,n}(t), \\ S_a(t) &= S_{a_n}(t) - Y_{7,n}(t), \quad E_a(t) = E_{a_n}(t) - Y_{8,n}(t), \quad I_a(t) = I_{a_n}(t) - Y_{9,n}(t), \end{aligned} \quad (12)$$

where $Y_{1,n}(t), Y_{2,n}(t), Y_{3,n}(t), Y_{4,n}(t), Y_{5,n}(t), Y_{6,n}(t), Y_{7,n}(t), Y_{8,n}(t), Y_{9,n}(t)$, illustrate the residual components of the series solutions. Therefore,

$$\begin{aligned} S_m(t) - S_{m_{n-1}}(t) &= \frac{2(1-\delta)J_1(S_m(t) - Y_{1,n}(t))}{M(\delta)(2-\delta)} + \frac{2\delta}{M(\delta)(2-\delta)} \int_0^t J_1(S_m(s) - Y_{1,n}(s))ds, \\ E_m(t) - E_{m_{n-1}}(t) &= \frac{2(1-\delta)J_2(E_m(t) - Y_{2,n}(t))}{M(\delta)(2-\delta)} + \frac{2\delta}{M(\delta)(2-\delta)} \int_0^t J_2(E_m(s) - Y_{2,n}(s))ds, \\ A_m(t) - A_{m_{n-1}}(t) &= \frac{2(1-\delta)J_3(A_m(t) - Y_{3,n}(t))}{M(\delta)(2-\delta)} + \frac{2\delta}{M(\delta)(2-\delta)} \int_0^t J_3(A_m(s) - Y_{3,n}(s))ds, \\ I_m(t) - I_{m_{n-1}}(t) &= \frac{2(1-\delta)J_4(I_m(t) - Y_{4,n}(t))}{M(\delta)(2-\delta)} + \frac{2\delta}{M(\delta)(2-\delta)} \int_0^t J_4(I_m(s) - Y_{4,n}(s))ds, \\ V_m(t) - V_{m_{n-1}}(t) &= \frac{2(1-\delta)J_5(V_m(t) - Y_{5,n}(t))}{M(\delta)(2-\delta)} + \frac{2\delta}{M(\delta)(2-\delta)} \int_0^t J_5(V_m(s) - Y_{5,n}(s))ds, \\ R_m(t) - R_{m_{n-1}}(t) &= \frac{2(1-\delta)J_6(R_m(t) - Y_{6,n}(t))}{M(\delta)(2-\delta)} + \frac{2\delta}{M(\delta)(2-\delta)} \int_0^t J_6(R_m(s) - Y_{6,n}(s))ds, \\ S_a(t) - S_{a_{n-1}}(t) &= \frac{2(1-\delta)J_7(S_a(t) - Y_{7,n}(t))}{M(\delta)(2-\delta)} + \frac{2\delta}{M(\delta)(2-\delta)} \int_0^t J_7(S_a(s) - Y_{7,n}(s))ds, \\ E_a(t) - E_{a_{n-1}}(t) &= \frac{2(1-\delta)J_8(E_a(t) - Y_{8,n}(t))}{M(\delta)(2-\delta)} + \frac{2\delta}{M(\delta)(2-\delta)} \int_0^t J_8(E_a(s) - Y_{8,n}(s))ds, \\ I_a(t) - I_{a_{n-1}}(t) &= \frac{2(1-\delta)J_9(I_a(t) - Y_{9,n}(t))}{M(\delta)(2-\delta)} + \frac{2\delta}{M(\delta)(2-\delta)} \int_0^t J_9(I_a(s) - Y_{9,n}(s))ds. \end{aligned} \quad (13)$$

By utilizing the norm on both sides and utilizing the Lipschitz principle, the preceding assertion results in

$$\begin{aligned} &\left\| S_m(t) - \frac{2(1-\delta)J_1(S_m(t), t)}{(2-\delta)M(\delta)} - S_m(0) - \frac{2\delta}{(2-\delta)M(\delta)} \int_0^t J_1(S_m(s), s)ds \right\| \\ &\leq \|Y_{1,n}(t)\| \left\{ 1 + \left(\frac{2(1-\delta)\xi_1}{(2-\delta)M(\delta)} + \frac{2\delta\xi_2 t}{(2-\delta)M(\delta)} \right) \right\}, \\ &\left\| E_m(t) - \frac{2(1-\delta)J_2(E_m(t), t)}{(2-\delta)M(\delta)} - E_m(0) - \frac{2\delta}{(2-\delta)M(\delta)} \int_0^t J_2(E_m(s), s)ds \right\| \\ &\leq \|Y_{2,n}(t)\| \left\{ 1 + \left(\frac{2(1-\delta)\xi_2}{(2-\delta)M(\delta)} + \frac{2\delta\xi_4 t}{(2-\delta)M(\delta)} \right) \right\}, \end{aligned}$$

$$\left\| A_m(t) - \frac{2(1-\delta)J_3(A_m(t), t)}{(2-\delta)M(\delta)} - A_m(0) - \frac{2\delta}{(2-\delta)M(\delta)} \int_0^t J_3(E_m(s), s) ds \right\|$$

$$\leq \|Y_{3,n}(t)\| \left\{ 1 + \left(\frac{2(1-\delta)\xi_5}{(2-\delta)M(\delta)} + \frac{2\delta\xi_6 t}{(2-\delta)M(\delta)} \right) \right\},$$

$$\left\| I_m(t) - \frac{2(1-\delta)J_4(I_m(t), t)}{(2-\delta)M(\delta)} - I_m(0) - \frac{2\delta}{(2-\delta)M(\delta)} \int_0^t J_4(I_m(s), s) ds \right\|$$

$$\leq \|Y_{4,n}(t)\| \left\{ 1 + \left(\frac{2(1-\delta)\xi_7}{(2-\delta)M(\delta)} + \frac{2\delta\xi_8 t}{(2-\delta)M(\delta)} \right) \right\},$$

$$\left\| V_m(t) - \frac{2(1-\delta)J_5(V_m(t), t)}{(2-\delta)M(\delta)} - V_m(0) - \frac{2\delta}{(2-\delta)M(\delta)} \int_0^t J_5(V_m(s), s) ds \right\|$$

$$\leq \|Y_{5,n}(t)\| \left\{ 1 + \left(\frac{2(1-\delta)\xi_9}{(2-\delta)M(\delta)} + \frac{2\delta\xi_{10} t}{(2-\delta)M(\delta)} \right) \right\},$$

$$\left\| R_m(t) - \frac{2(1-\delta)J_6(R_m(t), t)}{(2-\delta)M(\delta)} - R_m(0) - \frac{2\delta}{(2-\delta)M(\delta)} \int_0^t J_6(R_m(s), s) ds \right\|$$

$$\leq \|Y_{6,n}(t)\| \left\{ 1 + \left(\frac{2(1-\delta)\xi_{11}}{(2-\delta)M(\delta)} + \frac{2\delta\xi_{12} t}{(2-\delta)M(\delta)} \right) \right\},$$

$$\left\| S_a(t) - \frac{2(1-\delta)J_7(S_a(t), t)}{(2-\delta)M(\delta)} - S_a(0) - \frac{2\delta}{(2-\delta)M(\delta)} \int_0^t J_7(S_a(s), s) ds \right\|$$

$$\leq \|Y_{7,n}(t)\| \left\{ 1 + \left(\frac{2(1-\delta)\xi_{13}}{(2-\delta)M(\delta)} + \frac{2\delta\xi_{14} t}{(2-\delta)M(\delta)} \right) \right\},$$

$$\left\| E_a(t) - \frac{2(1-\delta)J_8(E_a(t), t)}{(2-\delta)M(\delta)} - E_a(0) - \frac{2\delta}{(2-\delta)M(\delta)} \int_0^t J_8(E_a(s), s) ds \right\|$$

$$\leq \|Y_{8,n}(t)\| \left\{ 1 + \left(\frac{2(1-\delta)\xi_{15}}{(2-\delta)M(\delta)} + \frac{2\delta\xi_{16} t}{(2-\delta)M(\delta)} \right) \right\},$$

$$\left\| I_a(t) - \frac{2(1-\delta)J_9(I_a(t), t)}{(2-\delta)M(\delta)} - I_a(0) - \frac{2\delta}{(2-\delta)M(\delta)} \int_0^t J_9(I_a(s), s)ds \right\|$$

$$\leq \|Y_{9,n}(t)\| \left\{ 1 + \left(\frac{2(1-\delta)\xi_{17}}{(2-\delta)M(\delta)} + \frac{2\delta\xi_{18}t}{(2-\delta)M(\delta)} \right) \right\}.$$

Following the implementation of *limit* as t procedures ∞ indicates that

$$\begin{aligned} S_m(t) &= \frac{2(1-\delta)J_1(S_m(t), t)}{M(\delta)(2-\delta)} + \frac{2\delta}{M(\delta)(2-\delta)} \int_0^t J_1(S_m(s), s)ds + S_m(0), \\ E_m(t) &= \frac{2(1-\delta)J_2(E_m(t), t)}{M(\delta)(2-\delta)} + \frac{2\delta}{M(\delta)(2-\delta)} \int_0^t J_2(E_m(s), s)ds + E_m(0), \\ A_m(t) &= \frac{2(1-\delta)J_3(A_m(t), t)}{M(\delta)(2-\delta)} + \frac{2\delta}{M(\delta)(2-\delta)} \int_0^t J_3(A_m(s), s)ds + A_m(0), \\ I_m(t) &= \frac{2(1-\delta)J_4(I_m(t), t)}{M(\delta)(2-\delta)} + \frac{2\delta}{M(\delta)(2-\delta)} \int_0^t J_4(I_m(s), s)ds + I_m(0), \\ V_m(t) &= \frac{2(1-\delta)J_5(V_m(t), t)}{M(\delta)(2-\delta)} + \frac{2\delta}{M(\delta)(2-\delta)} \int_0^t J_5(V_m(s), s)ds + V_m(0), \\ R_m(t) &= \frac{2(1-\delta)J_6(R_m(t), t)}{M(\delta)(2-\delta)} + \frac{2\delta}{M(\delta)(2-\delta)} \int_0^t J_6(R_m(s), s)ds + R_m(0), \\ S_a(t) &= \frac{2(1-\delta)J_7(S_a(t), t)}{M(\delta)(2-\delta)} + \frac{2\delta}{M(\delta)(2-\delta)} \int_0^t J_7(S_a(s), s)ds + S_a(0), \\ E_a(t) &= \frac{2(1-\delta)J_8(E_a(t), t)}{M(\delta)(2-\delta)} + \frac{2\delta}{M(\delta)(2-\delta)} \int_0^t J_8(E_a(s), s)ds + E_a(0), \\ I_a(t) &= \frac{2(1-\delta)J_9(I_a(t), t)}{M(\delta)(2-\delta)} + \frac{2\delta}{M(\delta)(2-\delta)} \int_0^t J_9(I_a(s), s)ds + I_a(0). \end{aligned}$$

This demonstrates the conclusion, indicating that the aforementioned are solutions of the model as specified by system (6).

Theorem 3 *The fractional order infectious disease model, as indicated by system (6), exhibits a unique solution.*

Proof Based on the principle of contradiction, we posit that $\left(S'_m(t), E'_m(t), A'_m(t), I'_m(t), V'_m(t), R'_m(t), S'_a(t), E'_a(t), I'_a(t) \right)$ it's additionally the solution to the developed fractional infectious disease model (6), consequently

$$\begin{aligned} S_m(t) - S'_m(t) &= \frac{2(1-\delta)\{J_1(S_m(t), t) - J_1(S'_m(t), t)\}}{(2-\delta)M(\delta)} \\ &\quad + \frac{2\delta}{(2-\delta)M(\delta)} \int_0^t \{J_1(S_m(s), s) - J_1(S'_m(s), s)\}ds, \end{aligned}$$

$$\begin{aligned}
E_m(t) - E'_m(t) &= \frac{2(1-\delta)\{J_2(E_m(t), t) - J_2(E'_m(t), t)\}}{(2-\delta)M(\delta)} \\
&\quad + \frac{2\delta}{(2-\delta)M(\delta)} \int_0^t \{J_2(E_m(s), s) - J_2(E'_m(s), s)\} ds, \\
A_m(t) - A'_m(t) &= \frac{2(1-\delta)\{J_3(A_m(t), t) - J_3(A'_m(t), t)\}}{(2-\delta)M(\delta)} \\
&\quad + \frac{2\delta}{(2-\delta)M(\delta)} \int_0^t \{J_3(A_m(s), s) - J_3(A'_m(s), s)\} ds, \\
I_m(t) - I'_m(t) &= \frac{2(1-\delta)\{J_4(I_m(t), t) - J_4(I'_m(t), t)\}}{(2-\delta)M(\delta)} \\
&\quad + \frac{2\delta}{(2-\delta)M(\delta)} \int_0^t \{J_4(I_m(s), s) - J_4(I'_m(s), s)\} ds, \\
V_m(t) - V'_m(t) &= \frac{2(1-\delta)\{J_5(V_m(t), t) - J_5(V'_m(t), t)\}}{(2-\delta)M(\delta)} \\
&\quad + \frac{2\delta}{(2-\delta)M(\delta)} \int_0^t \{J_5(V_m(s), s) - J_5(V'_m(s), s)\} ds, \\
R_m(t) - R'_m(t) &= \frac{2(1-\delta)\{J_6(R_m(t), t) - J_6(R'_m(t), t)\}}{(2-\delta)M(\delta)} \\
&\quad + \frac{2\delta}{(2-\delta)M(\delta)} \int_0^t \{J_6(R_m(s), s) - J_6(R'_m(s), s)\} ds, \\
S_a(t) - S'_a(t) &= \frac{2(1-\delta)\{J_7(S_a(t), t) - J_7(S'_a(t), t)\}}{(2-\delta)M(\delta)} \\
&\quad + \frac{2\delta}{(2-\delta)M(\delta)} \int_0^t \{J_7(S_a(s), s) - J_7(S'_a(s), s)\} ds, \\
E_a(t) - E'_a(t) &= \frac{2(1-\delta)\{J_8(E_a(t), t) - J_8(E'_a(t), t)\}}{(2-\delta)M(\delta)} \\
&\quad + \frac{2\delta}{(2-\delta)M(\delta)} \int_0^t \{J_8(E_a(s), s) - J_8(E'_a(s), s)\} ds, \\
I_a(t) - I'_a(t) &= \frac{2(1-\delta)\{J_9(I_a(t), t) - J_9(I'_a(t), t)\}}{(2-\delta)M(\delta)} \\
&\quad + \frac{2\delta}{(2-\delta)M(\delta)} \int_0^t \{J_9(I_a(s), s) - J_9(I'_a(s), s)\} ds.
\end{aligned}$$

Based on the property of majorizing, we can express the aforementioned system as

$$\begin{aligned}
\|S_m(t) - S'_m(t)\| &\leq \frac{2(1-\delta)\|J_1(S_m(t), t) - J_1(S'_m(t), t)\|}{(2-\delta)M(\delta)} \\
&\quad + \frac{2\delta}{(2-\delta)M(\delta)} \int_0^t \|J_1(S_m(s), s) - J_1(S'_m(s), s)\| ds, \\
\|E_m(t) - E'_m(t)\| &\leq \frac{2(1-\delta)\|J_2(E_m(t), t) - J_2(E'_m(t), t)\|}{(2-\delta)M(\delta)} \\
&\quad + \frac{2\delta}{(2-\delta)M(\delta)} \int_0^t \|J_2(E_m(s), s) - J_2(E'_m(s), s)\| ds,
\end{aligned}$$

$$\begin{aligned}
\|A_m(t) - A'_m(t)\| &\leq \frac{2(1-\delta)\|J_3(A_m(t), t) - J_3(A'_m(t), t)\|}{(2-\delta)M(\delta)} \\
&\quad + \frac{2\delta}{(2-\delta)M(\delta)} \int_0^t \|J_3(A_m(s), s) - J_3(A'_m(s), s)\| ds, \\
\|I_m(t) - I'_m(t)\| &\leq \frac{2(1-\delta)\|J_4(I_m(t), t) - J_4(I'_m(t), t)\|}{(2-\delta)M(\delta)} \\
&\quad + \frac{2\delta}{(2-\delta)M(\delta)} \int_0^t \|J_4(I_m(s), s) - J_4(I'_m(s), s)\| ds, \\
\|V_m(t) - V'_m(t)\| &\leq \frac{2(1-\delta)\|J_5(V_m(t), t) - J_5(V'_m(t), t)\|}{(2-\delta)M(\delta)} \\
&\quad + \frac{2\delta}{(2-\delta)M(\delta)} \int_0^t \|J_5(V_m(s), s) - J_5(V'_m(s), s)\| ds, \\
\|R_m(t) - R'_m(t)\| &\leq \frac{2(1-\delta)\|J_6(R_m(t), t) - J_6(R'_m(t), t)\|}{(2-\delta)M(\delta)} \\
&\quad + \frac{2\delta}{(2-\delta)M(\delta)} \int_0^t \|J_6(R_m(s), s) - J_6(R'_m(s), s)\| ds, \\
\|S_a(t) - S'_a(t)\| &\leq \frac{2(1-\delta)\|J_7(S_a(t), t) - J_7(S'_a(t), t)\|}{(2-\delta)M(\delta)} \\
&\quad + \frac{2\delta}{(2-\delta)M(\delta)} \int_0^t \|J_7(S_a(s), s) - J_7(S'_a(s), s)\| ds, \\
\|E_a(t) - E'_a(t)\| &\leq \frac{2(1-\delta)\|J_8(E_a(t), t) - J_8(E'_a(t), t)\|}{(2-\delta)M(\delta)} \\
&\quad + \frac{2\delta}{(2-\delta)M(\delta)} \int_0^t \|J_8(E_a(s), s) - J_8(E'_a(s), s)\| ds, \\
\|I_a(t) - I'_a(t)\| &\leq \frac{2(1-\delta)\|J_9(I_a(t), t) - J_9(I'_a(t), t)\|}{(2-\delta)M(\delta)} \\
&\quad + \frac{2\delta}{(2-\delta)M(\delta)} \int_0^t \|J_9(I_a(s), s) - J_9(I'_a(s), s)\| ds.
\end{aligned}$$

By applying the findings established in (1) and (2), we achieve

$$\begin{aligned}
\|S_m(t) - S'_m\| &\leq \frac{2\zeta_1\zeta_1(1-\delta)}{(2-\delta)M(\delta)} + \left(\frac{2\zeta_2\delta\zeta_2t}{M(\delta)(2-\delta)} \right)^n, \\
\|E_m(t) - E'_m\| &\leq \frac{2\zeta_3\zeta_3(1-\delta)}{(2-\delta)M(\delta)} + \left(\frac{2\zeta_4\delta\zeta_4t}{M(\delta)(2-\delta)} \right)^n, \\
\|A_m(t) - A'_m\| &\leq \frac{2\zeta_5\zeta_5(1-\delta)}{(2-\delta)M(\delta)} + \left(\frac{2\zeta_6\delta\zeta_6t}{M(\delta)(2-\delta)} \right)^n, \\
\|I_m(t) - I'_m\| &\leq \frac{2\zeta_7\zeta_7(1-\delta)}{(2-\delta)M(\delta)} + \left(\frac{2\zeta_8\delta\zeta_8t}{M(\delta)(2-\delta)} \right)^n, \\
\|V_m(t) - V'_m\| &\leq \frac{2\zeta_9\zeta_9(1-\delta)}{(2-\delta)M(\delta)} + \left(\frac{2\zeta_{10}\delta\zeta_{10}t}{M(\delta)(2-\delta)} \right)^n,
\end{aligned} \tag{14}$$

$$\begin{aligned}
\|R_m(t) - R'_m\| &\leq \frac{2\tilde{\zeta}_{11}\zeta_{11}(1-\delta)}{(2-\delta)M(\delta)} + \left(\frac{2\tilde{\zeta}_{12}\delta\zeta_{12}t}{M(\delta)(2-\delta)} \right)^n, \\
\|S_a(t) - S'_a\| &\leq \frac{2\tilde{\zeta}_{13}\zeta_{13}(1-\delta)}{(2-\delta)M(\delta)} + \left(\frac{2\tilde{\zeta}_{14}\delta\zeta_{14}t}{M(\delta)(2-\delta)} \right)^n, \\
\|E_a(t) - E'_a\| &\leq \frac{2\tilde{\zeta}_{15}\zeta_{15}(1-\delta)}{(2-\delta)M(\delta)} + \left(\frac{2\tilde{\zeta}_{16}\delta\zeta_{16}t}{M(\delta)(2-\delta)} \right)^n, \\
\|I_a(t) - I'_a\| &\leq \frac{2\tilde{\zeta}_{17}\zeta_{17}(1-\delta)}{(2-\delta)M(\delta)} + \left(\frac{2\tilde{\zeta}_{18}\delta\zeta_{18}t}{M(\delta)(2-\delta)} \right)^n.
\end{aligned}$$

The inequalities presented in Eq. (14) are valid for all values of n , leading us to the conclusion

$$\begin{aligned}
S_m(t) &= S'_m(t), \quad E_m(t) = E'_m(t), \quad A_m(t) = A'_m(t), \quad I_m(t) = I'_m(t), \quad V_m(t) = V'_m(t), \\
R_m(t) &= R'_m(t), \quad S_a(t) = S'_a(t), \quad E_a(t) = E'_a(t), \quad I_a(t) = I'_a(t).
\end{aligned} \tag{15}$$

The Lipschitz condition is pivotal in ensuring the uniqueness of the solution by guaranteeing that small variations in the initial conditions or parameters lead to proportionally small changes in the solution. Intuitively, this condition prevents the system from exhibiting erratic or unpredictable behavior, which is critical when modeling real-world disease dynamics. In this work, the context of Mpox transmission, the Lipschitz condition ensures that the predicted number of infections remains stable and consistent under slight perturbations in the transmission or recovery rates. This stability is vital for reliable disease modeling and control strategies. By enforcing a bounded rate of change, the Lipschitz condition acts as a safeguard against anomalies, ensuring the mathematical and practical robustness of the model.

4 Equilibra and fundamental reproduction number

The Mpox-free equilibrium corresponds to the case when no infections exist within the population. The derivations of the equilibrium points Ψ^0 and Ψ^* , it is important to note their practical implications in understanding disease dynamics. The disease-free equilibrium Ψ^0 represents a scenario where the disease is eradicated from the population, with all infected compartments at zero. This presents the critical role of intervention strategies, such as vaccination and public health measures, in achieving and maintaining a disease-free state. In contrast, the endemic equilibrium Ψ^* corresponds to a persistent state of the disease within the population. The proportions of infected individuals at Ψ^* depend on parameters such as contact rates, recovery rates, and vaccination efficacy. This underscores the significance of controlling the reproduction number R_0 and modifying key parameters to shift the system toward the disease-free equilibrium. These insights provide actionable guidance for policymakers and public health officials in formulating strategies to manage and potentially eliminate Mpox outbreaks.

Hence, the Mpox free equilibrium point

$$\begin{aligned}
\Psi^0 &= (S_m^0, E_m^0, A_m^0, I_m^0, V_m^0, R_m^0, S_a^0, E_a^0, I_a^0) \\
&= \left(\frac{c_5\Pi_m}{(c_1c_5 - \alpha_m\tau) + c_5\lambda_m}, 0, 0, 0, \frac{\alpha_m\Pi_m}{(c_1c_5 - \alpha_m\tau) + c_5\lambda_m}, 0, \frac{\Pi_a}{\mu_2}, 0, 0 \right).
\end{aligned}$$

The endemic equilibrium of Mpox is $\Psi^* = (S_m^*, E_m^*, A_m^*, I_m^*, V_m^*, R_m^*, S_a^*, E_a^*, I_a^*)$. Then, from system (6) the endemic equilibrium points are

$$\begin{aligned} S_m^* &= \frac{c_5 \Pi_m}{(c_1 c_5 - \alpha_m \tau) + c_5 \lambda_m}, & E_m^* &= \frac{\lambda_m^* S_m^*}{c_2}, & A_m^* &= \frac{k(1-\rho) E_m^*}{c_4}, & I_m^* &= \frac{k \rho E_m^*}{c_3}, \\ V_m^* &= \frac{\alpha_m \Pi_m}{(c_1 c_5 - \alpha_m \tau) + c_5 \lambda_m}, & R_h^* &= \frac{k(1-\rho) c_5 \gamma_1 \lambda_m \Pi_m}{c_2 c_4 ((c_1 c_5 - \alpha_m \tau) + c_5 \lambda_m)} + \frac{k \rho c_5 \gamma_2 \lambda_m \Pi_m}{c_2 c_3 ((c_1 c_5 - \alpha_m \tau) + c_5 \lambda_m)}, \\ S_a^* &= \frac{\Pi_a (\pi + c_7)}{(c_6 c_7 (\frac{\beta_4 \pi}{C_6 c_7} - 1) + \mu_2 (\pi + c_7))}, & E_a^* &= \frac{\Pi_a c_7 (\frac{\beta_4 \pi}{C_6 c_7} - 1)}{(c_6 c_7 (\frac{\beta_4 \pi}{C_6 c_7} - 1) + \mu_2 (\pi + c_7))}, \\ I_a^* &= \frac{\pi \Pi_a (\frac{\beta_4 \pi}{C_6 c_7} - 1)}{(c_6 c_7 (\frac{\beta_4 \pi}{C_6 c_7} - 1) + \mu_2 (\pi + c_7))}, \end{aligned}$$

where

$$\begin{aligned} c_1 &= (\mu_1 + \alpha_m), \quad c_2 = (\mu_1 + k), \quad c_3 = (\gamma_2 + \mu_1 + \eta_1), \quad c_4 = (\gamma_1 + \mu_1 + \eta_2), \\ c_5 &= (\tau + \mu_1), \quad c_6 = (\pi + \mu_2), \quad c_7 = (\mu_2 + \eta_3), \quad \lambda_m = \left(\frac{\beta_1 I_m^* + \beta_2 I_a^* + \beta_3 A_m^*}{N_m} \right). \end{aligned}$$

The fundamental reproduction number of the human and rodent population Mpox model (6) is computed via the next-generation matrix. Using this technique [21], we have

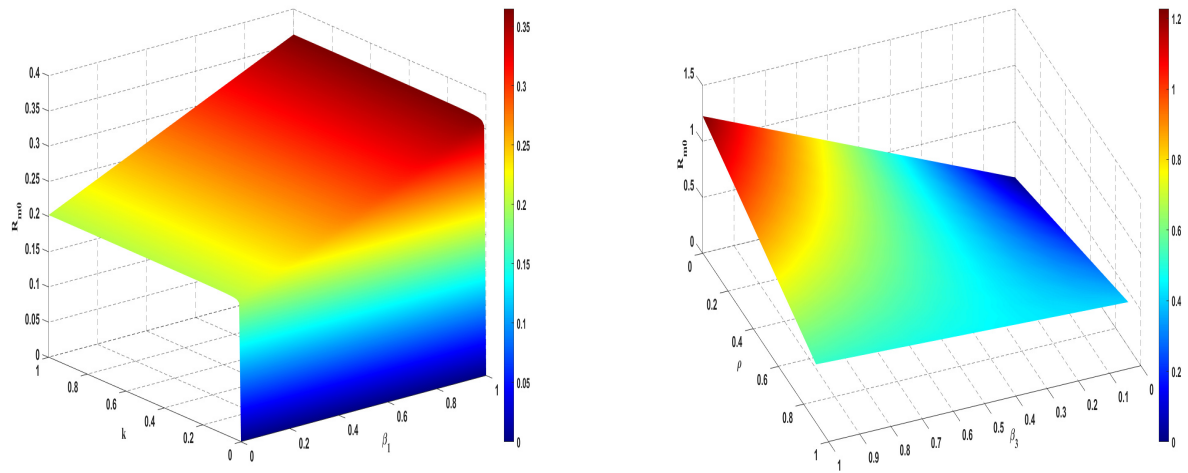
$$F = \begin{bmatrix} 0 & \frac{S_m^0 \beta_1}{N_m^0} & \frac{S_m^0 \beta_3}{N_m^0} & 0 & 0 & \frac{S_m^0 \beta_2}{N_m^0} \\ 0 & 0 & 0 & 0 & 0 & 0 \\ 0 & 0 & 0 & 0 & 0 & 0 \\ 0 & 0 & 0 & 0 & 0 & 0 \\ 0 & 0 & 0 & 0 & 0 & \beta_4 \\ 0 & 0 & 0 & 0 & 0 & 0 \end{bmatrix}, \quad V = \begin{bmatrix} c_2 & 0 & 0 & 0 & 0 & 0 \\ -k\rho & c_3 & 0 & 0 & 0 & 0 \\ -k(1-\rho) & 0 & c_4 & 0 & 0 & 0 \\ 0 & 0 & 0 & c_5 & 0 & 0 \\ 0 & 0 & 0 & 0 & c_6 & 0 \\ 0 & 0 & 0 & 0 & -\pi & c_7 \end{bmatrix}.$$

The reproduction number is the dominant eigenvalue of FV^{-1} . Thus,

$$R_0 = \max\{R_{m_0}, R_{a_0}\} = \max \left\{ \frac{kc_5(\beta_1 \rho c_4 + \beta_3(1-\rho)c_3)}{c_2 c_3 c_4 (\alpha_m + c_5)}, \frac{\beta_4 \pi}{c_6 c_7} \right\}. \quad (16)$$

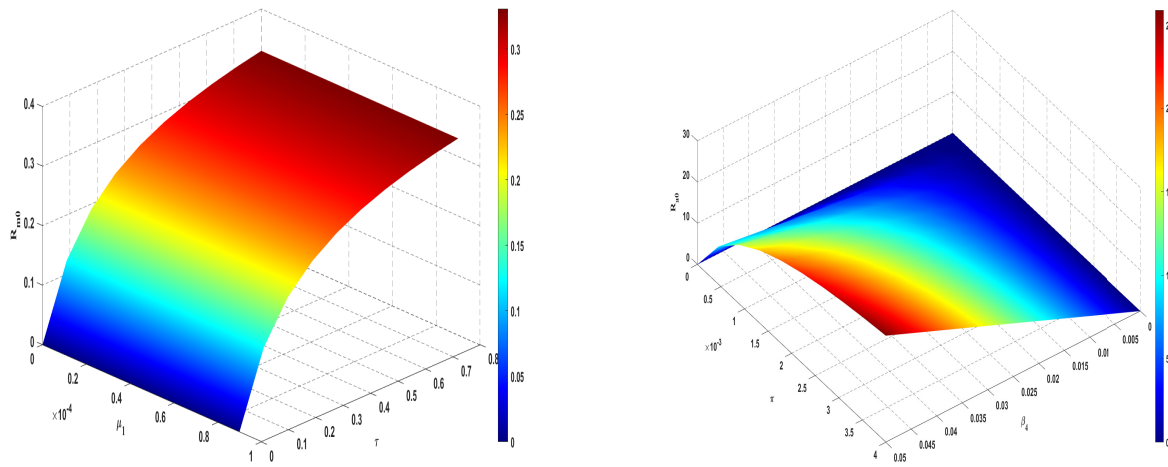
The fundamental reproduction number R_0 is a pivotal metric in understanding the spread of infectious diseases. The Mpox model's R_0 depends on several parameters, such as contact rates, transmission probabilities, recovery rates, and others as outlined in Eq. (16). Additionally, these Figure 2 and Figure 3 illustrate the effect of different parameter combinations of the examining the influencing the fundamental reproduction numbers of humans R_{m_0} and rodent R_{a_0} . The interplay of these factors determines whether the disease will spread ($R_0 > 1$) or decline ($R_0 < 1$). To ensure effective control, policies should target reducing R_0 to below 1. Vaccinating a substantial fraction of the population is estimated to be at least 75% of the total susceptible individuals based on model outputs. Implementing social distancing and minimizing inter-species transmission pathways to reduce contact rates. Also, enhancing recovery rates through early diagnosis and treatment programs. This analysis underlines the importance of targeted interventions on specific

parameters to control the spread of Mpox.



(a) Dynamical behaviour of R_{m0} for β_1 and k values (b) Dynamical behaviour of R_{m0} for β_3 and ρ values

Figure 2. Dynamical behaviour of R_{m0} for different variables



(a) Dynamical behaviour of R_{m0} for μ_1 and τ values (b) Dynamical behaviour of R_{a0} for β_4 and π values

Figure 3. Dynamical behaviour of R_{m0} and R_{a0} for different variables

5 Numerical simulations

Numerical method

This section of the study presents an estimated approach to addressing the fractional order Mpox model (6) utilizing the two-step fractional Adams-Bashforth approach for the CF fractional derivative [22]. The structure is implemented using the fractional Volterra model, which is based on the basic theorem of integration. This method offers a balance between computational efficiency and accuracy, making it well-suited for iterative simulations involving fractional derivatives. The choice of the Adams-Bashforth method is rooted in its ability to handle the memory effect inherent

in fractional models, as it builds on previous computational steps to predict future values. This iterative approach aligns well with the characteristics of the Caputo-Fabrizio derivative used in our model, ensuring stability and precision in the simulations. Specifically, the method's compatibility with non-local properties of fractional calculus enhances its capability to simulate long-term interactions and dynamic responses. In order to achieve the required iterative strategy, we first focus just on the first equation of system (6) and follow the steps shown below. Utilizing the basic concept of integration, we derive the subsequent outcome from the initial equation of the system (7).

$$S_m(t) - S_m(0) = \frac{(1-\delta)}{M(\delta)} J_1(t, S_m) + \frac{\delta}{M(\delta)} \int_0^t J_1(x, S_m) dx. \quad (17)$$

For $t = t_{n+1}, n = 0, 1, 2, \dots$, we acquire

$$S_m(t_{n+1}) - S_{m_0} = \frac{(1-\delta)}{M(\delta)} J_1(t, S_m) + \frac{\delta}{M(\delta)} \int_0^{t_{n+1}} J_1(x, S_m) dx. \quad (18)$$

The difference between each consecutive term is shown as follows:

$$S_{m_{n+1}} - S_{m_n} = \frac{1-\delta}{M(\delta)} \{J_1(t_n, S_{m_n}) - J_1(t_{n-1}, S_{m_{n-1}})\} + \frac{\delta}{M(\delta)} \int_{t_n}^{t_{n+1}} J_1(t, S_m) dt. \quad (19)$$

Over the close interval $[t_k, t_{(k+1)}]$, the function $J_1(t, S_m)$ is able to estimated using the interpolation polynomial

$$\mathcal{H}_k \cong \frac{f(t_k, y_k)}{h} (t - t_{k-1}) - \frac{f(t_{k-1}, y_{k-1})}{h} (t - t_k),$$

where $h = t_n - t_{n-1}$. The integral in (19) is computed using the polynomial estimation outlined above, resulting in

$$\begin{aligned} \int_{t_n}^{t_{n+1}} J_1(t, S_m) dt &= \int_{t_n}^{t_{n+1}} \left(\frac{J_1(t_n, S_{m_n})}{h} - \frac{J_1(t_{n-1}, S_{m_{n-1}})}{h} (t - t_n) \right) dt \\ &= \frac{3h}{2} J_1(t_n, S_{m_n}) - \frac{n}{2} J_1(t_{n-1}, S_{m_{n-1}}). \end{aligned} \quad (20)$$

Putting (20) in (19) and after simplification we acquire

$$S_{m_{n+1}} = S_{m_n} + \left(\frac{1-\delta}{M(\delta)} + \frac{3h}{2M(\delta)} \right) J_1(t_n, S_{m_n}) - \left(\frac{1-\delta}{M(\delta)} + \frac{\delta h}{2M(\delta)} \right) J_1(t_{n+1}, S_{m_{n-1}}). \quad (21)$$

Similar to this, we were able to derive the recursive formulas for the other equations in system (7) as follows

$$\begin{aligned} E_{m_{n+1}} &= E_{m_n} + \left(\frac{1-\delta}{M(\delta)} + \frac{3h}{2M(\delta)} \right) J_2(t_n, E_{m_n}) - \left(\frac{1-\delta}{M(\delta)} + \frac{\delta h}{2M(\delta)} \right) J_2(t_{n+1}, E_{m_{n-1}}), \\ A_{m_{n+1}} &= A_{m_n} + \left(\frac{1-\delta}{M(\delta)} + \frac{3h}{2M(\delta)} \right) J_3(t_n, A_{m_n}) - \left(\frac{1-\delta}{M(\delta)} + \frac{\delta h}{2M(\delta)} \right) J_3(t_{n+1}, A_{m_{n-1}}), \end{aligned}$$

$$\begin{aligned}
I_{m_{n+1}} &= I_{m_n} + \left(\frac{1-\delta}{M(\delta)} + \frac{3h}{2M(\delta)} \right) J_4(t_n, I_{m_n}) - \left(\frac{1-\delta}{M(\delta)} + \frac{\delta h}{2M(\delta)} \right) J_4(t_{n+1}, I_{m_{n-1}}), \\
V_{m_{n+1}} &= V_{m_n} + \left(\frac{1-\delta}{M(\delta)} + \frac{3h}{2M(\delta)} \right) J_5(t_n, V_{m_n}) - \left(\frac{1-\delta}{M(\delta)} + \frac{\delta h}{2M(\delta)} \right) J_5(t_{n+1}, V_{m_{n-1}}), \quad (22) \\
R_{m_{n+1}} &= R_{m_n} + \left(\frac{1-\delta}{M(\delta)} + \frac{3h}{2M(\delta)} \right) J_6(t_n, R_{m_n}) - \left(\frac{1-\delta}{M(\delta)} + \frac{\delta h}{2M(\delta)} \right) J_6(t_{n+1}, R_{m_{n-1}}), \\
S_{a_{n+1}} &= S_{a_n} + \left(\frac{1-\delta}{M(\delta)} + \frac{3h}{2M(\delta)} \right) J_7(t_n, S_{a_n}) - \left(\frac{1-\delta}{M(\delta)} + \frac{\delta h}{2M(\delta)} \right) J_7(t_{n+1}, S_{a_{n-1}}), \\
E_{a_{n+1}} &= E_{a_n} + \left(\frac{1-\delta}{M(\delta)} + \frac{3h}{2M(\delta)} \right) J_8(t_n, E_{a_n}) - \left(\frac{1-\delta}{M(\delta)} + \frac{\delta h}{2M(\delta)} \right) J_8(t_{n+1}, E_{a_{n-1}}), \\
I_{a_{n+1}} &= I_{a_n} + \left(\frac{1-\delta}{M(\delta)} + \frac{3h}{2M(\delta)} \right) J_9(t_n, I_{a_n}) - \left(\frac{1-\delta}{M(\delta)} + \frac{\delta h}{2M(\delta)} \right) J_9(t_{n+1}, I_{a_{n-1}}).
\end{aligned}$$

Furthermore, we present the numerical simulations conducted to examine the interactions of the proposed model, as indicated in system (6), for different values of δ , random sequence of CF derivative throughout the range of $[0, 1]$, as well as for other model relevant factors.

6 Discussion

The objective of the numerical simulation is to examine the effects of changes in order and parameters are shown in the Table 1 on the dynamic behavior of the system. To create Figure 4–Figure 14, we use the utilizing two-step fractional Adams-Bashforth technique [22] of the CF derivative.

Table 1. The values of the model parameters

Parameter	Explanation	Values	Source
Π_m	Recruitment into susceptible humans	64850	[1]
Π_a	Recruitment into susceptible rodent	0.2	[8]
β_1	Rate of S_m and contagious rodent	0.3632	$0 < \beta_1 \leq 1$
β_2	Rate of S_m and contagious humans	0.4192	$0 < \beta_2 \leq 1$
β_3	Rate of A_m from susceptible humans	0.1900	[23]
β_4	Rate of S_a and contagious rodent	0.1802	[23]
α_m	Vaccination rate from the susceptible humans	0.2104	Fitted
τ	Waning rate of induced immunity	0.3525	[23]
k	Rate of transition of E_m to infected human	0.3966	$0 < k \leq 1$
ρ	Exposure-related infection rate	0.132	$0 < \rho \leq 1$
γ_1	Recovery rate from A_m	0.5093	Assumed
γ_2	Recovery rate from infected humans	0.5093	Fitted
π	Infected rodent to exposed rodents rate	0.5410	$0 < \pi \leq 1$
μ_1	Natural morality rate of humans	0.000303	[1]
μ_2	Natural morality rate of rodents	0.0012	Assumed
η_1	Death rate of A_m due to Mpox	4.1187×10^{-4}	Fitted
η_2	Death rate of I_m due to Mpox	0.0012	[23]
η_3	Death rate of I_a due to Mpox	2.8532×10^{-4}	Fitted

Figure 4 shows the density of susceptible human populations over time (t) at various values of the fractional order δ . The values of δ likely represent different scenarios in the model, affecting how the susceptible population changes over time. Figure 5 represents the population density of individuals who have been exposed to the illness but have not yet become contagious. The numerous graphs represent different values of δ , illustrating the temporal fluctuations in exposure levels.

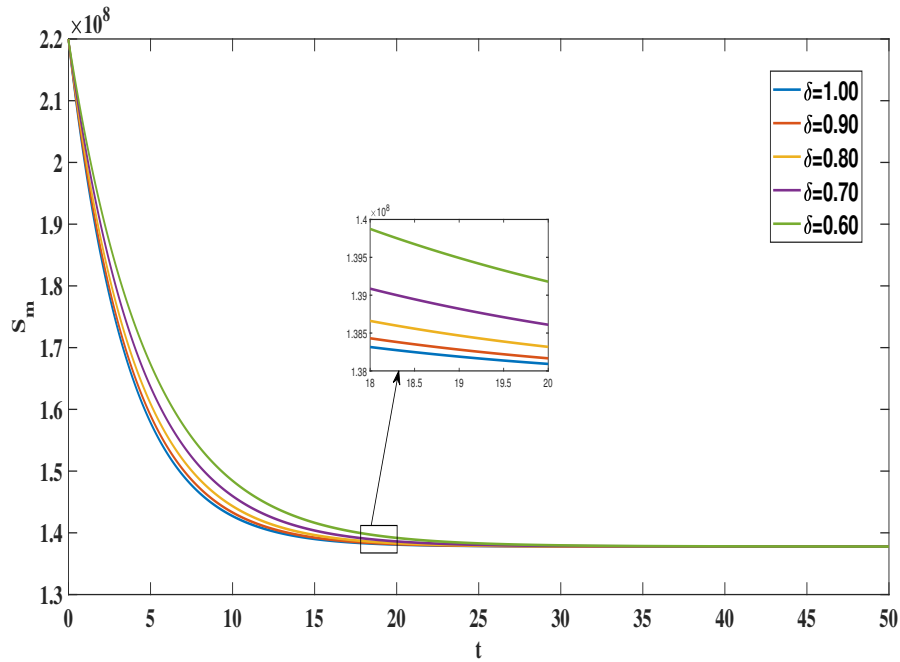


Figure 4. Population density of suspected human populations at different values δ

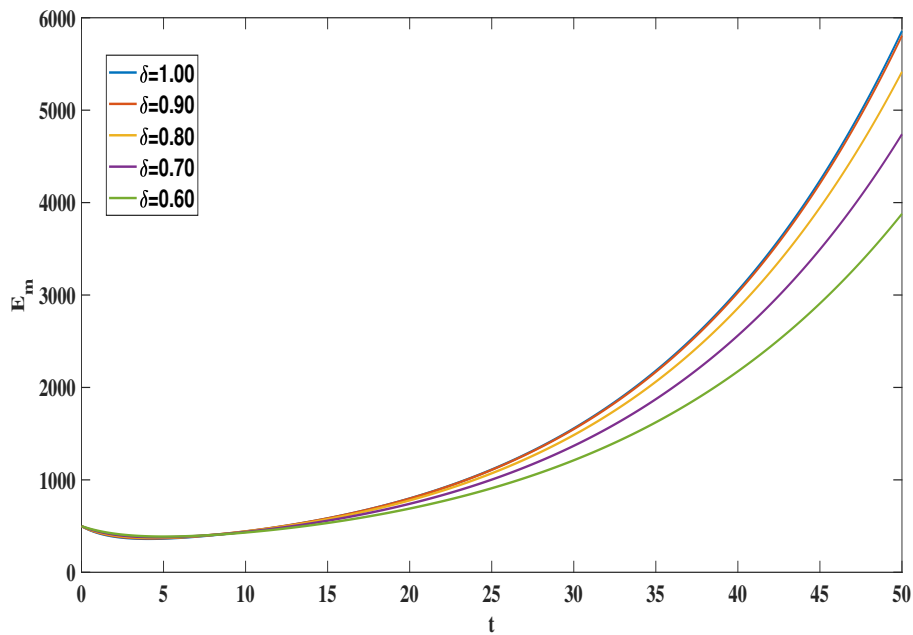


Figure 5. Population density of exposed humans populations at different values δ

Figure 6 focuses on the asymptomatic but infected human population. The different δ values show how this segment of the population varies over time t , indicating the impact of different model parameters on asymptomatic infection rates. Figure 7 shows the density of humans who are actively infected. The variation in δ values allows for the comparison of infection trends under different fractional orders as represented by δ .

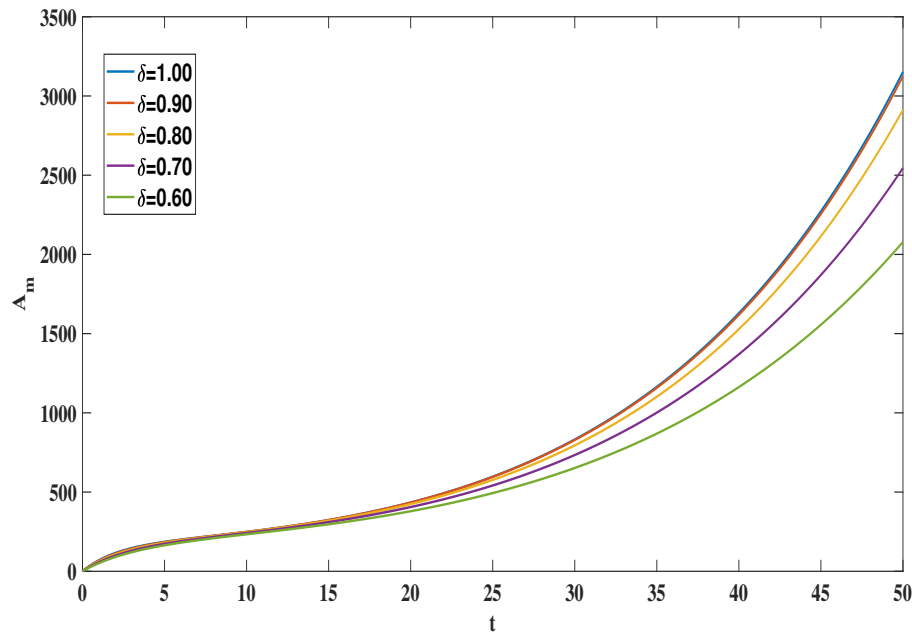


Figure 6. Population density of asymptotically-ill human populations at different values δ

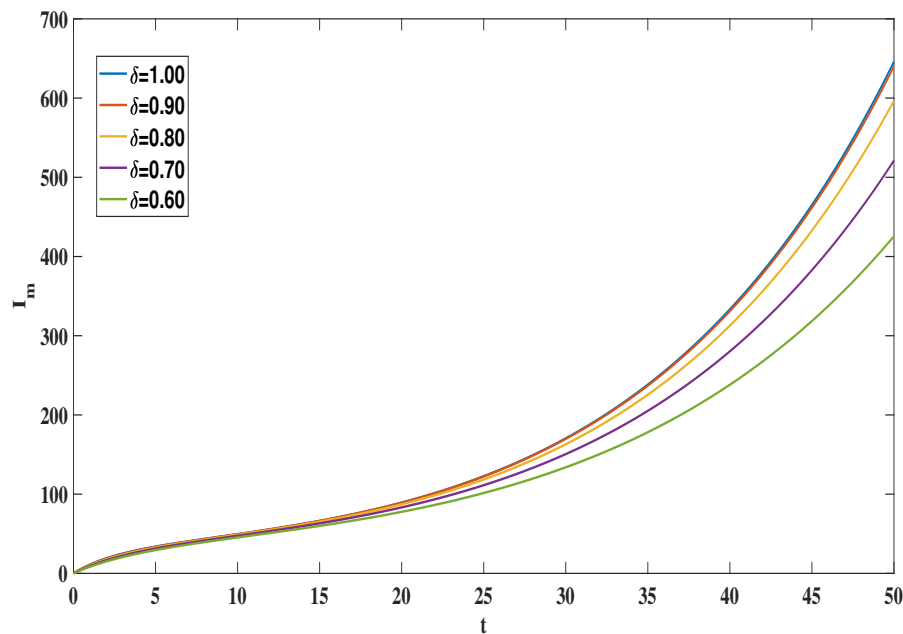


Figure 7. Population density of infected human populations at different values δ

The **Figure 8** illustrates the population density of humans who have been vaccinated. The various δ values likely represent different vaccination rates or efficacies, showing how vaccination impacts the population over time t . **Figure 9** presents the density of humans who have recovered from the infection. The different δ values depict how recovery rates and the number of recovered individuals evolve under different scenarios.

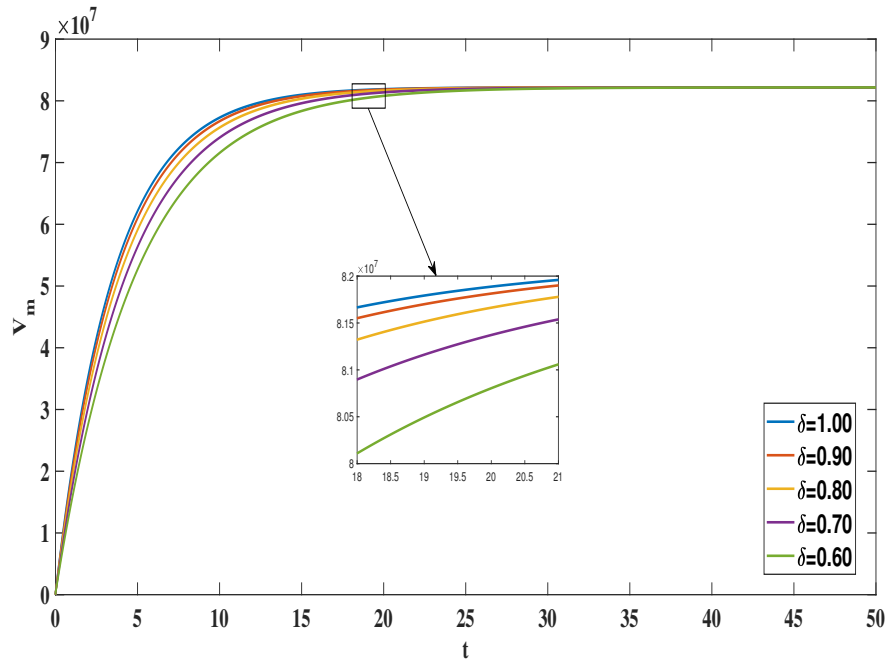


Figure 8. Population density of vaccinated human populations at different values δ

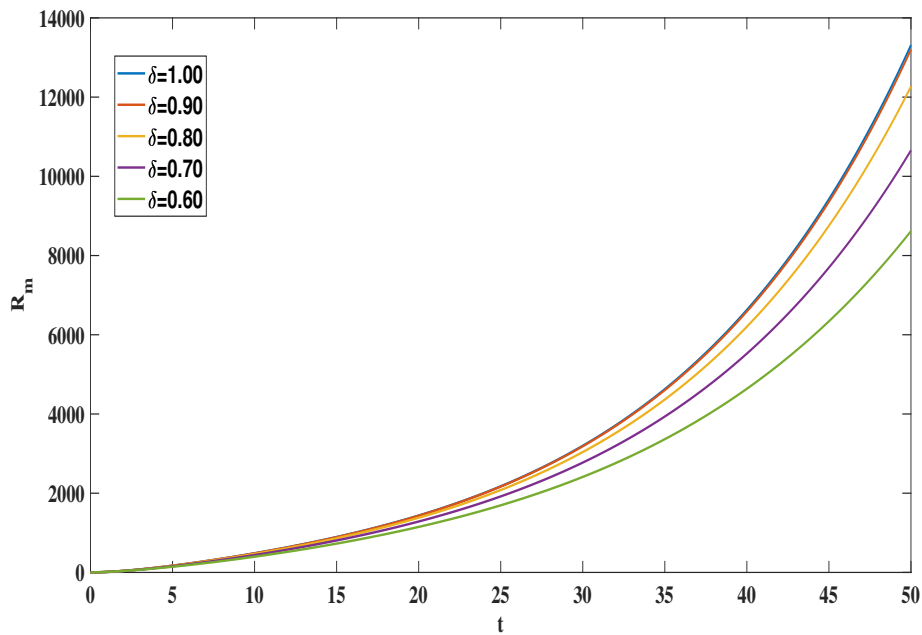


Figure 9. Population density of recovered human populations at different values δ

Figure 10 shows the population density of rodents suspected to be susceptible to the disease. The fractional order δ indicates different scenarios or intervention strategies affecting this population over time. Figure 11 illustrates the population density of exposed rodent populations. The different δ values demonstrate how exposure among rodents changes over time under various conditions. Figure 12 depicts the density of actively infected rodent populations. The variations in δ values show how infection spreads within the rodent population.

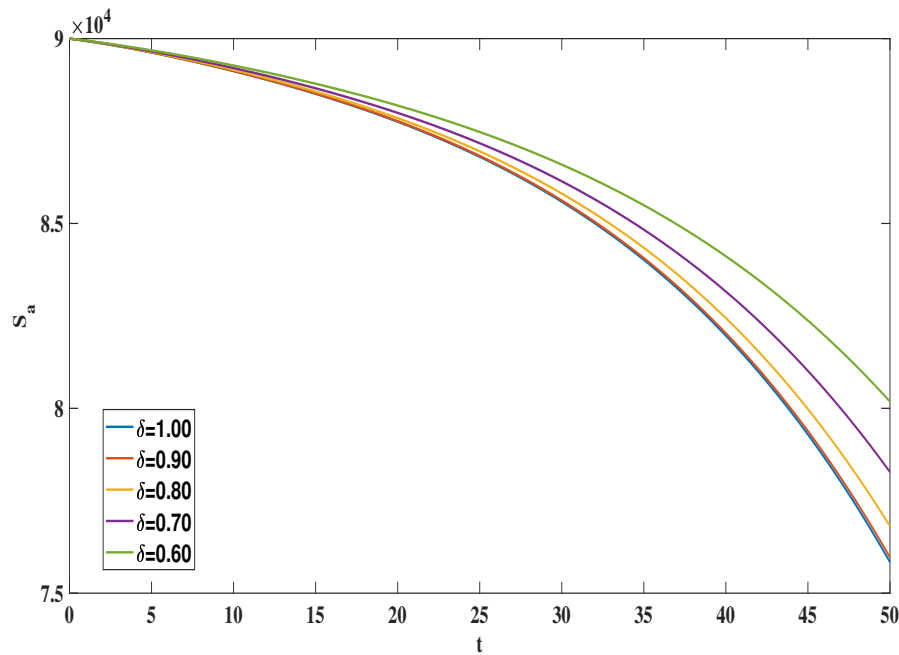


Figure 10. Population density of suspected rodent populations at different values δ

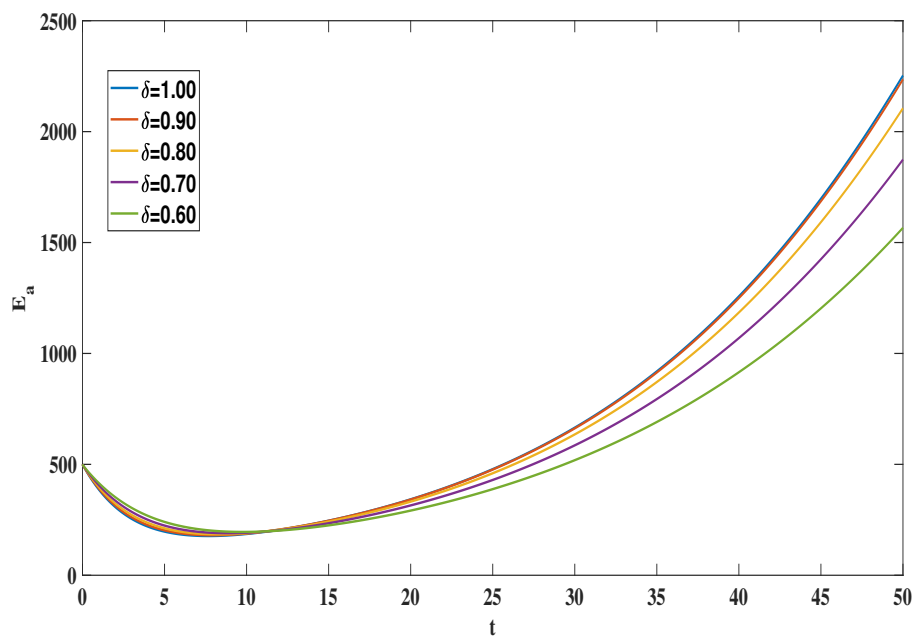


Figure 11. Population density of exposed rodent populations at different values δ

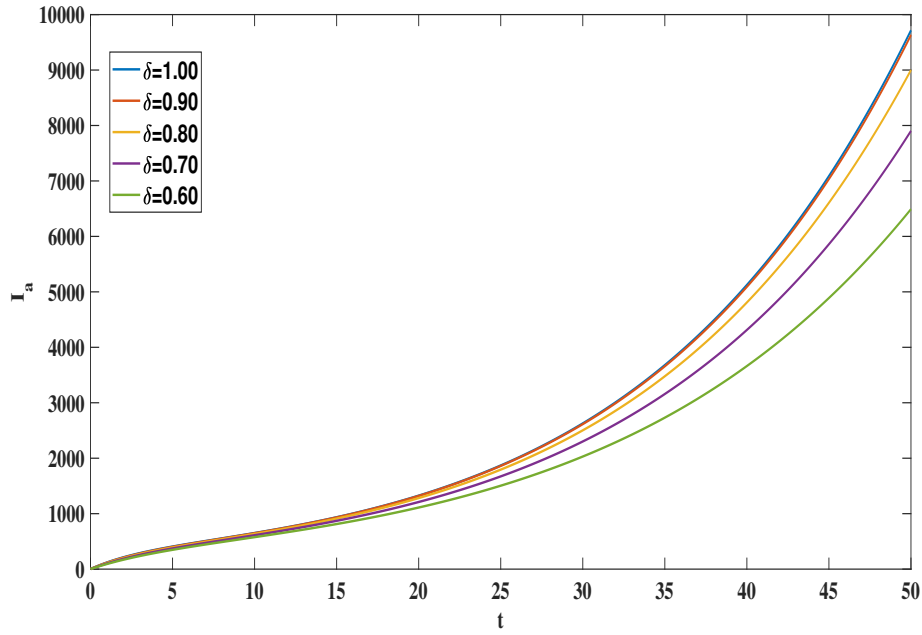
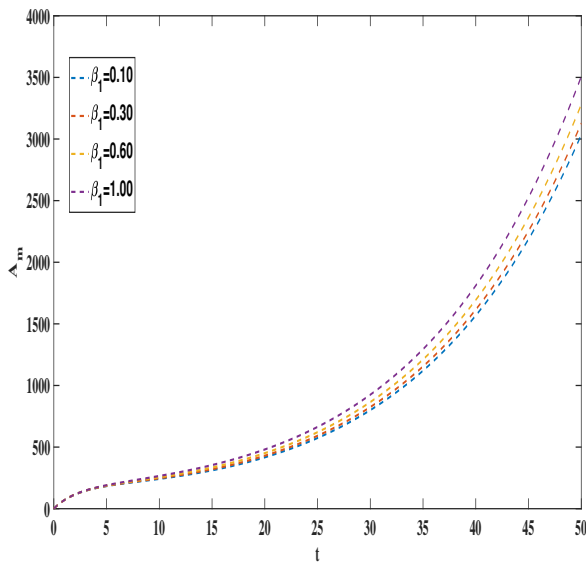
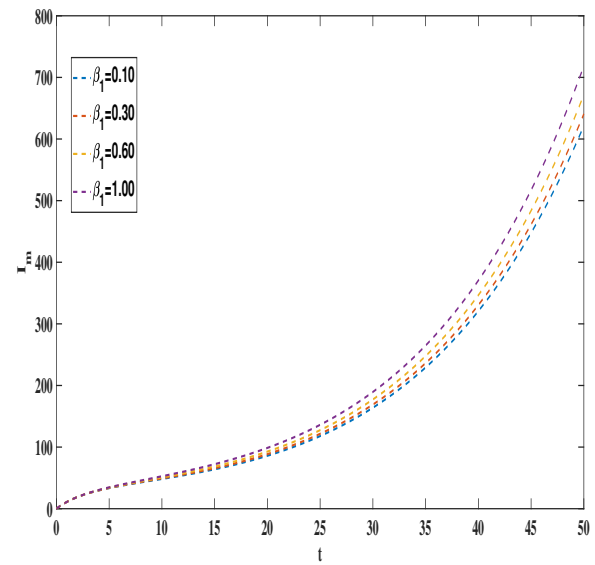


Figure 12. Population density of infected rodent populations at different values δ

From **Figure 13** to **Figure 16** appear to show the results of numerical simulations that explore the dynamics of a proposed model asymptotically-ill A_m humans and infected I_m humans for Mpox transmission. Specifically, this figure likely illustrates how varying a key parameter, denoted respectively $\beta_1, \beta_3, \beta_4$ affects certain population densities or infection rates over time t .



(a) Dynamical behavior of A_m at different values of β_1



(b) Dynamical behaviour of I_m at different values of β_1

Figure 13. Graphical representations of A_m and I_m for β_1

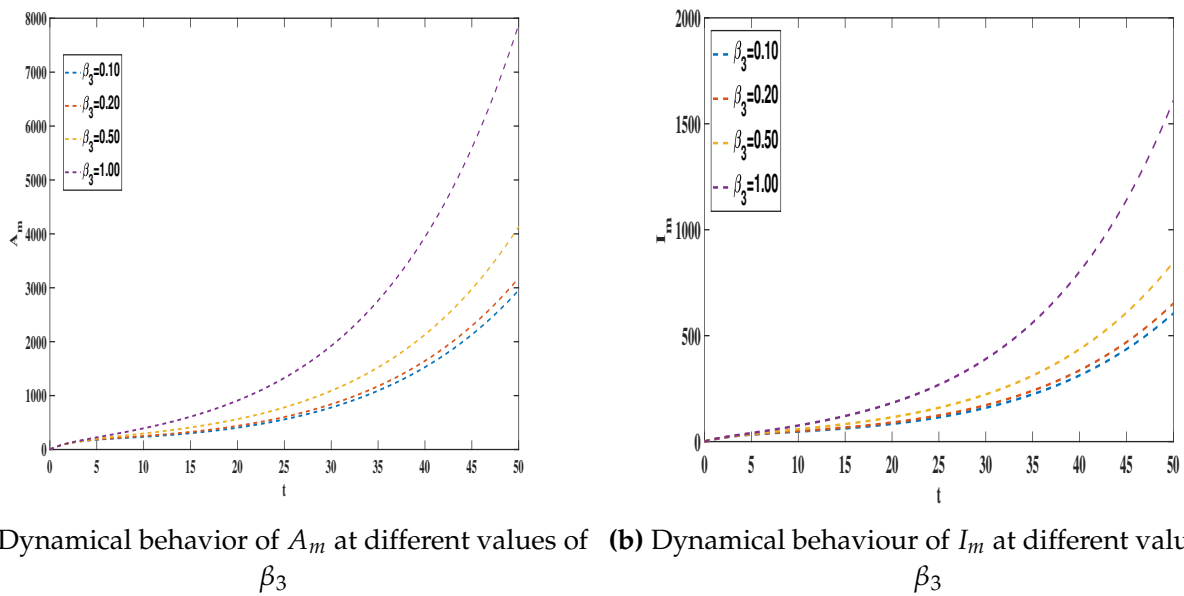


Figure 14. Graphical representations of A_m and I_m for β_3

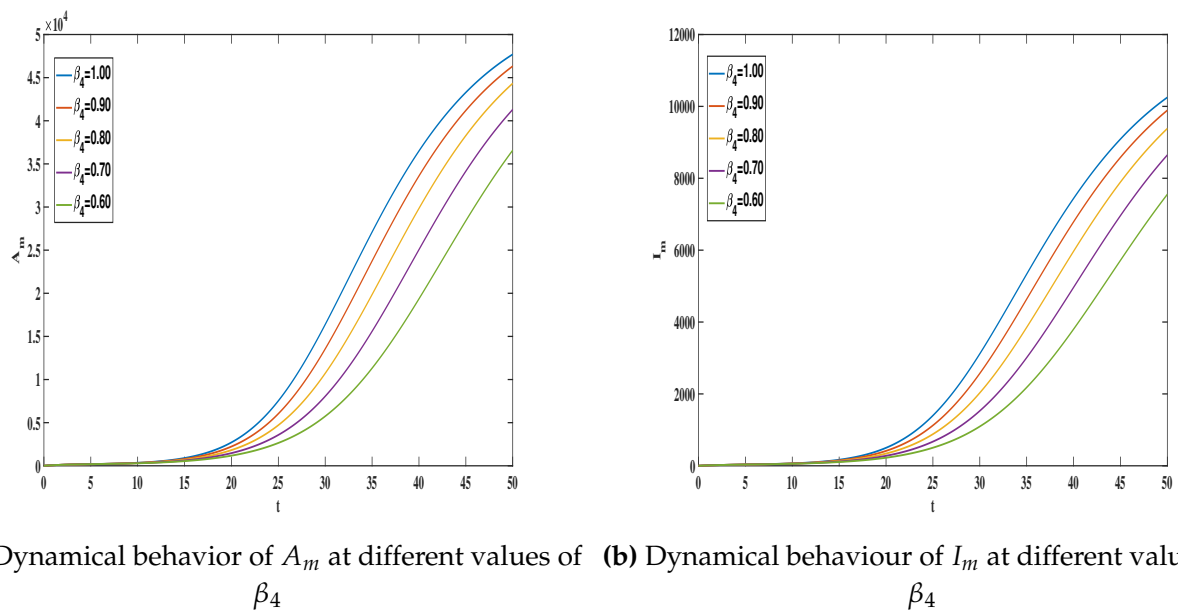
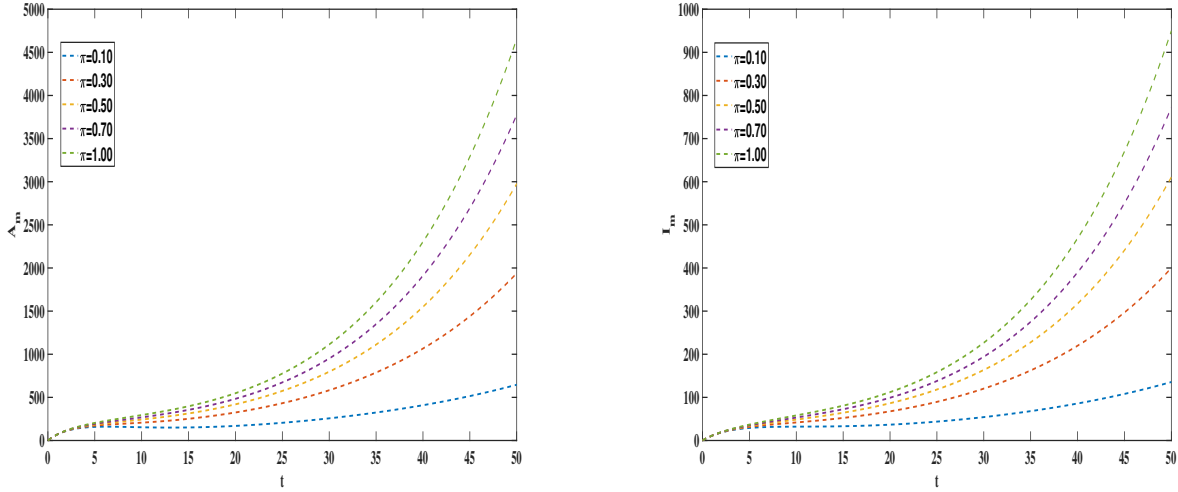


Figure 15. Graphical representations of A_m and I_m for β_4

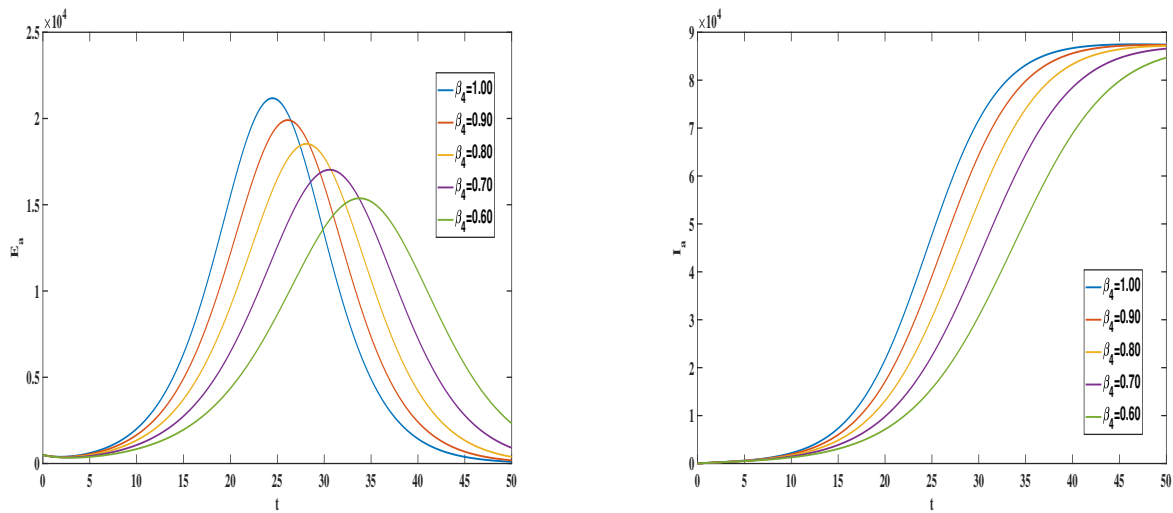
Figure 16 presents the outcomes of numerical simulations that investigate the dynamics of a proposed model involving asymptotically-ill A_m and infected I_m in the context of Mpox transmission. This figure likely demonstrates the impact of altering a key parameter, represented by π , on specific population densities or infection rates as time t progresses.

The model employs the CF fractional derivative, which is a mathematical tool used to describe processes with memory or hereditary properties. Simulations using numerical methods are conducted to analyze the dynamics of the model as outlined in system (6). The iterative technique of the CF derivative is used to generate the data for these figures.



(a) Dynamical behavior of A_m at different values of π (b) Dynamical behaviour of I_m at different values of π

Figure 16. Graphical representations of A_m and I_m for π



(a) Dynamical behaviour of E_a for β_4 values (b) Dynamical behavior of I_a at different values of β_4

Figure 17. Graphical representations of E_a and I_a for β_4

Figure 17 continues from Figure 15 by showing additional or comparative results of the numerical simulations under different β_4 values. This figure might depict another aspect of the model's behavior, such as the transition rates between different compartments of the model (e.g., susceptible, exposed, infected) over time t . The focus on different β_4 values helps in understanding the sensitivity of the model to changes in this fractional order, which is crucial for validating the model's robustness and reliability in predicting Mpox dynamics under varying conditions.

The CF fractional model captures memory and hereditary properties in epidemiological systems. This feature aligns well with the observed transmission dynamics of Mpox, which may involve delayed responses in immunity and disease progression. The solutions demonstrate consistency across a range of fractional orders δ . Notably, the choice of $\delta = 0.60, 0.70, 0.80, 0.90, 1.00$ appeared to yield slightly more accurate alignment with empirical data. The value of δ significantly impacts

the rate of infection spread and recovery, as it controls the degree of memory effect incorporated into the model.

7 Conclusion

In this investigation, we formulated a fractional-order epidemiological framework to examine the dynamics of the Mpox virus transmission, incorporating both symptomatic and asymptomatic infections. The model was rigorously analyzed for the existence and uniqueness of solutions, demonstrating that it possesses a unique solution under certain conditions. The key findings demonstrate the impact of vaccination rates, contact rates, and immunity waning on the basic reproduction number (R_0) and the disease's spread within human and rodent populations. The synergistic effect of the human-to-human transmission rate (β_1) and the progression rate of exposed individuals (k) significantly elevates the human reproduction number (R_{m_0}), while increased vaccination rates (α_m) and reduced immunity waning (τ) contribute to a decline in R_{m_0} . Similarly, in rodents, the interaction between the infected-to-susceptible contact rate (β_4) and the progression rate of exposed rodents (π) critically affects the rodent reproduction number R_{a_0} . Numerical simulations were conducted to validate the theoretical findings, showing that the model accurately captures the spread of the virus and the impact of various parameters on the infection dynamics. The results highlight the critical role of asymptomatic individuals in the transmission of Mpox and underscore the importance of targeted control measures. This work provides a valuable framework for understanding the complex dynamics of Mpox and can inform public health strategies for managing outbreaks. Future studies could benefit from localized modeling efforts. Also, the model has been validated using simulated datasets, but the incorporation of real epidemiological data could improve the robustness of our findings and validate assumptions made regarding disease progression and intervention strategies.

Declarations

Use of AI tools

The authors declare that they have not used Artificial Intelligence (AI) tools in the creation of this article.

Data availability statement

There are no data associated with this article

Ethical approval (optional)

The authors state that this research complies with ethical standards. This research does not involve either human participants or animals.

Consent for publication

Not applicable

Conflicts of interest

The authors declare that they have no conflict of interest.

Funding

No funding was received for this research.

Author's contributions

M.M.: Conceptualization, Writing-Original draft preparation, Investigation, Methodology, Software, Visualization. A.V.: Writing - Review & Editing, Formal Analysis, Supervision. S.K.: Software, Validation, Writing-Reviewing and Editing. All authors discussed the results and contributed to the final manuscript.

Acknowledgements

Not applicable

References

- [1] Worldometer, United States Population, (2022). <https://www.worldometers.info/world-population/us-population/>
- [2] Centers for Disease Control and Prevention (CDC), What You Should Know About Monkeypox, (2022). <https://www.cdc.gov/poxvirus/monkeypox/>
- [3] World Health Organization (WHO), Monkeypox, (2022). <https://www.who.int/news-room/factsheets/detail/Mpox>
- [4] Bunge, E.M., Hoet, B., Chen, L., Lienert, F., Weidenthaler, H., Baer, L.R. and Steffen, R. The changing epidemiology of human monkeypox-A potential threat? A systematic review. *PLoS Neglected Tropical Diseases*, 16(2), e0010141, (2022). [[CrossRef](#)]
- [5] Bhattar, S., Jangid, K., Abidemi, A., Owolabi, K.M. and Purohit, S.D. A new fractional mathematical model to study the impact of vaccination on COVID-19 outbreaks. *Decision Analytics Journal*, 6, 100156, (2023). [[CrossRef](#)]
- [6] Jose, S.A., Yaagoub, Z., Joseph, D., Ramachandran, R. and Jirawattanapanit, A. Computational dynamics of a fractional order model of chickenpox spread in Phuket province. *Biomedical Signal Processing and Control*, 91, 105994, (2024). [[CrossRef](#)]
- [7] Okyere, S. and Ackora-Prah, J. Modeling and analysis of monkeypox disease using fractional derivatives. *Results in Engineering*, 17, 100786, (2023). [[CrossRef](#)]
- [8] Peter, O.J., Kumar, S., Kumari, N., Oguntolu, F.A., Oshinubi, K. and Musa, R. Transmission dynamics of Monkeypox virus: a mathematical modelling approach. *Modeling Earth Systems and Environment*, 8, 3423–3434, (2022). [[CrossRef](#)]
- [9] Venkatesh, A., Manivel, M. and Baranidharan, B. Numerical study of a new time-fractional Mpox model using Caputo fractional derivatives. *Physica Scripta*, 99(2), 025226, (2024). [[Cross-Ref](#)]
- [10] Manivel, M., Venkatesh, A., Arunkumar, K., Prakash Raj, M. and Shyamsunder. A mathematical model of the dynamics of the transmission of monkeypox disease using fractional differential equations. *Advanced Theory and Simulations*, 7(9), 2400330, (2024). [[CrossRef](#)]
- [11] Venkatesh, A., Manivel, M., Arunkumar, K., Prakash Raj, M., Shyamsunder and Purohit, S.D. A fractional mathematical model for vaccinated humans with the impairment of Monkeypox transmission. *European Physical Journal Special Topics*, (2024). [[CrossRef](#)]
- [12] Bozkurt, F., Baleanu, D. and Bilgil, H. A mathematical model of mobility-related infection and vaccination in an epidemiological case. *Computer Methods in Biomechanics and Biomedical Engineering*, 1-21, (2024). [[CrossRef](#)]
- [13] Öztürk, Z., Bilgil, H. and Sorgun, S. Application of fractional SIQRV model for SARS-CoV-2 and stability analysis. *Symmetry*, 15(5), 1048, (2023). [[CrossRef](#)]

- [14] Öztürk, Z., Yousef, A., Bilgil, H. and Sorgun, S. A Fractional-order mathematical model to analyze the stability and develop a sterilization strategy for the habitat of stray dogs. *An International Journal of Optimization and Control: Theories & Applications*, 14(2), 134-146, (2024). [[CrossRef](#)]
- [15] Jothika, S. and Radhakrishnan, M. Dynamics of an SIR pandemic model using constrained medical resources with time delay. *Communications in Mathematical Biology and Neuroscience*, 2023, 90, (2023). [[CrossRef](#)]
- [16] Bankuru, S.V., Kossol, S., Hou, W., Mahmoudi, P., Rychtář, J. and Taylor, D. A game-theoretic model of Monkeypox to assess vaccination strategies. *PeerJ*, 8, e9272, (2020). [[CrossRef](#)]
- [17] Manivel, M., Venkatesh, A., Kumar, K.A., Raj, M.P., Fadugba, S.E. and Kekana, M. Quantitative modeling of monkeypox viral transmission using Caputo fractional variational iteration method. *Partial Differential Equations in Applied Mathematics*, 13, 101026, (2025). [[CrossRef](#)]
- [18] Usman, S. and Adamu, I.I. Modeling the transmission dynamics of the monkeypox virus infection with treatment and vaccination interventions. *Journal of Applied Mathematics and Physics*, 5(12), 2335-2353, (2017). [[CrossRef](#)]
- [19] Caputo, M. and Fabrizio, M. A new definition of fractional derivative without singular kernel. *Progress in Fractional Differentiation & Applications*, 1(2), 73-85, (2015). [[CrossRef](#)]
- [20] Losada, J. and Nieto, J.J. Properties of a new fractional derivative without singular kernel. *Progress in Fractional Differentiation and Applications*, 1(2), 87-92, (2015). [[CrossRef](#)]
- [21] Van den Driessche, P. and Watmough, J. Reproduction numbers and sub-threshold endemic equilibria for compartmental models of disease transmission. *Mathematical Biosciences*, 180(1-2), 29-48, (2002). [[CrossRef](#)]
- [22] Atangana, A. and Owolabi, K.M. New numerical approach for fractional differential equations. *Mathematical Modelling of Natural Phenomena*, 13(1), 3, (2018). [[CrossRef](#)]
- [23] Li, S., Ullah, S., AlQahtani, S.A., Tag, S.M. and Akgül, A. Mathematical assessment of Monkeypox with asymptomatic infection: Prediction and optimal control analysis with real data application. *Results in Physics*, 51, 106726, (2023). [[CrossRef](#)]

Mathematical Modelling and Numerical Simulation with Applications (MMNSA)
<https://dergipark.org.tr/en/pub/mmnsa>



Copyright: © 2025 by the authors. This work is licensed under a Creative Commons Attribution 4.0 (CC BY) International License. The authors retain ownership of the copyright for their article, but they allow anyone to download, reuse, reprint, modify, distribute, and/or copy articles in MMNSA, so long as the original authors and source are credited. To see the complete license contents, please visit (<http://creativecommons.org/licenses/by/4.0/>).

How to cite this article: Manivel, M., Venkatesh, A. & Kumawat, S. (2025). A comprehensive study of monkeypox disease through fractional mathematical modeling. *Mathematical Modelling and Numerical Simulation with Applications*, 5(1), 65-96. <https://doi.org/10.53391/mmnsa.1571609>